Application of ground-based InSAR for rock slope monitoring and site assessment at the Checkerboard Creek Rock Slope

by

Adam Woods

A thesis submitted in partial fulfillment of the requirements for the degree of

Master of Science

in

Geotechnical Engineering

Department of Civil and Environmental Engineering
University of Alberta

ABSTRACT

In recent years ground-based, interferometric, synthetic aperture radar (GB-InSAR) has been successfully implemented for purposes of monitoring displacements of both natural and man-made slopes. GB-InSAR monitoring has also provided detailed, spatially continuous, and high temporal frequency datasets that can be analyzed to provide further insights into key aspects of slope movements including its deformation mechanism(s), spatial extents of landslide activity, and other aspects of landslide kinematics. However, despite these capabilities, this technology has seen limited use within North America and Canada outside of the mining industry due to a variety of factors ranging from associated equipment costs, perceived technical limitations, and unfamiliarity of geoscience and engineering professionals with resulting data, analysis and interpretation.

Therefore, to test the applicability of this technology on natural slopes with conditions that are typical to many landslide sites in North America and Canada which include features such as dense vegetation cover, mountainous terrain, deep seasonal snowpack, and inclement weather, it has been applied at a known 2 to 3 million m^3 bedrock landslide site with a very slow-average displacement rate (~10 mm/y) known as The Checkerboard Creek Rock Slope located near Revelstoke, BC, Canada. To assess GB-InSAR's ability to monitor this site and to quantify its potential advantages over traditional geotechnical monitoring techniques and other remote sensing technologies (such as satellite-based InSAR, LiDAR, GNSS, and UAV photogrammetry) resulting temporally discontinuous datasets have been analysed and validated, compared, and contrasted against historical in-place instrumentation data.

Additionally, identification and mitigation of the logistical challenges and technical limitations associated with the initial installation of the GB-InSAR equipment at the Checkerboard Creek Rock Slope and site conditions were completed as part of this research which included the expansion of the solar power system, installation of telecommunications equipment for remote access to operating software and collected data, and improvement of the coverage and quality of

the GB-InSAR data by means of installation of corner point reflectors, new radar antennas, and shelter window. An analysis of the key limitation of GB-InSAR and other similar technologies due to vegetation and snow ground cover was completed as part of this research and concluded that compensating for apparent movements from snow accumulation and melt can be successfully implemented by making resulting discontinuously processed InSAR displacements relative to a known stable area. However, GB-InSAR results in areas of dense vegetation remain unreliable, therefore, analysis of future data collected with the system improvements made at site such as corner point reflectors is recommended to further evaluate this limitation of the application of this technology at natural slope landslide site.

GB-InSAR monitoring equipment at this site was also used to develop new insights into multiple aspects of the Checkerboard Creek Rock Slope. These insights included further confirmation of the currently understood deformation mechanism of complex rotational toppling, in addition to an updated understanding of slope deformation characteristics such as refinement of the northern extent of the active zone of movement, indication that the seasonal pattern in displacement rates recorded by near-surface in-place instruments may be at least partially due to thermal effects on the instruments themselves rather than due to real ground movements, and possible identification of new previously unidentified areas of potential slope movement.

PREFACE

This is a "paper-format" style dissertation. Chapters 2 and 3 are either submitted for publication or published as detailed below. Versions of the individual manuscripts as presented in this thesis may differ slightly from the published versions.

Chapter 2 is published in the May 2020 edition of the International Consortium on Landslides (Landslides), titled GB-InSAR monitoring of vegetated and snow-covered slopes in remote mountainous environments (Wood et al. 2020).

Chapter 3 was submitted as a journal manuscript, titled Updated understanding of the deformation characteristics of the Checkerboard Creek rock slope in Canada, through GB-InSAR monitoring. This paper has been shortened and revised to fit the requirements for submission to the journal Engineering Geology on May 2020 (Woods et al. Submitted).

I was responsible for all data analysis, data interpretation, discussion, and manuscript composition. Dr. M.T. Hendry and Dr. R. Macciotta were involved in data collection, developing the concept for the dissertation, and as supervisors; each has reviewed all parts of the work. T. Stewart and J. Marsh of BC Hydro also contributed to the direction of this research and reviewed the published works found in Chapters 2 and 3.

Dedication

To my parents, Buffie and Nigel, for always supporting me in my education and for without them, this document would not exist.

ACKNOWLEDGEMENTS

I'd like to thank my supervisors, Dr. Michael Hendry and Dr. Renato Macciotta for their consistent support, guidance, and patience throughout the entirety of my graduate degree and in the process of creating this document. This research was made possible through the (Canadian) Railway Ground Hazard Research Program (RGHRP), which is funded by the Natural Sciences and Engineering Research Council of Canada (CRDPJ 470162-14), Canadian Pacific Railway and Canadian National Railway. The authors would also like to thank BC Hydro, and specifically Tom Stewart and Julia Marsh with their Dam Safety Department at the Revelstoke Dam in Revelstoke BC, and their instrumentation technician staff, for their support in installing, maintaining, and upgrading of the GB-InSAR system and sharing their vast experience and knowledge of the Checkerboard Creek Rock Slope site. Technical assistance regarding the GB-InSAR system and associated software was provided by IDS Georadar's North American office, namely David Manthei, John Metzgar, and Jake Davidson. Drs. Derek Martin and Doug Stead also provided many additional insights.

TABLE OF CONTENTS

1 INTRODUCTION ... 1

1.1 Background ... 1

1.2 Scope and Objectives ... 4

2 PAPER 1: GB-InSAR monitoring of vegetated and snow-covered slopes in remote mountainous environments ... 15

2.1 Introduction ... 15

2.2 Ground-based InSAR ... 16

2.2.1 Fundamentals and Applications ... 16

2.2.2 Limitations and Logistical Challenges ... 18

2.2.3 Available Solutions ... 20

2.3 Addressing the Challenges of GB-InSAR at the Checkerboard Creek Rock Slope ... 22

2.3.1 Site Description ... 22

2.3.2 Instrumentation and Other Monitoring ... 25

2.3.3 Checkerboard Creek GB-InSAR Installation ... 27

2.4 Data Processing and Validation ... 30

2.4.1 Data Collection ... 30

2.4.2 Validation of GB-InSAR Results ... 31

2.4.3 Statistical Analysis of GB-InSAR Results and Sources of Error ... 33

2.4.4 Impact of Snow Accumulation and Melt ... 35

2.5 Conclusions ... 38

3 PAPER 2: Insights into Checkerboard Creek Rock Slope deformations using GB-InSAR monitoring under challenging conditions ... 40

3.1 Introduction ... 40

3.2 The Checkerboard Creek Rock Slope ... 41

3.2.1 Site History 44

3.2.2 Site Geology 44

3.2.3 Groundwater Conditions 45

3.2.4 Site Climatic Conditions 46

3.2.5 Slope Displacement Trends 46

3.2.6 In-place Instrumentation 48

3.3 Slope Stability Modelling 49

3.3.1 Preliminary Numerical Modelling (FLAC) 50

3.3.2 Discrete Element Analysis (UDEC) 50

3.3.3 Damage Model (UDEC-DM) 52

3.4 GB-InSAR Monitoring 53

3.4.1 Installation Details 55

3.4.2 Continuous Data (C-InSAR) 58

3.4.3 Discontinuous Data (D-InSAR) 59

3.5 Results 60

3.5.1 Deformation Mode Confirmation (Toppling) 60

3.5.2 Seasonal Displacement Pattern 62

3.5.3 Spatial Extent of Active Slope Movement 68

3.5.4 Upper Vegetated Area of Slope 73

3.6 Conclusions 73

4 CONCLUSIONS AND RECOMMENDATIONS 75

4.1 Recommendations for Further Research 78

References 81

LIST OF TABLES

Table 2-1: Monitoring Technique Summary 17

Table 2-2: Instrumentation Summary 26

Table 2-3: GB-InSAR accessory cost breakdown 29

Table 2-4: Snow accumulation and melt impact of GB-InSAR results 36

Table 3-1: GB-InSAR Monitoring Campaign Details 54

Table 3-2: Seasonal Variation of GB-InSAR at Select Instrumentation Locations 64

LIST OF FIGURES

Figure 2-1: GB-InSAR components as at Checkerboard Creek Rock Slope installation (photograph taken by A.Woods, May 2018). 19

Figure 2-2: Radar corner point reflector on tripod mount (a) and mounted on rock face (b) (photograph courtesy of IDS Georadar) 21

Figure 2-3: Location of the Checkerboard Creek Rock Slope and GB-InSAR installation. 23

Figure 2-4: Typical geological cross-section of Checkerboard Creek Rock Slope and related in-place instrumentation (after Watson et al. 2006). 24

Figure 2-5: Drillhole (CC1 to CC11) and surface cable extensometer locations (LiDAR hillshade image generated from 2014 BC Hydro survey). 27

Figure 2-6: Original solar panel installation Oct. 2016 to Oct. 2018 (a) and battery pack and 20 A charge controller (b). Upgraded solar installation Oct. 2018 to present (c) and insulated aluminum battery boxes (d). 28

Figure 2-7: Checkerboard Creek GB-InSAR detailed solar power system and telecommunications schematic 29

Figure 2-8: GB-InSAR cumulative LoS displacement map between November 15, 2016 and March 4, 2019. Locations of extensometer CC10 and slope inclinometer CC4 are noted. 32

Figure 2-9: Cumulative displacement in LoS direction by discontinuous GB-InSAR in the vicinity of extensometer CC10 (a) and slope inclinometer CC4 (b) and average displacement of nearby survey monuments. 33

Figure 2-10: Statistical analysis of GB-InSAR results. 35

Figure 2-11: Impact of snow accumulation and melt on apparent LoS displacement 37

Figure 2-12: Accumulated precipitation over winter months vs. apparent movement of stable area 38

Figure 3-1: Checkerboard Creek Rock Slope Elevation viewed from west side of Revelstoke Reservoir 42

Figure 3-2: Drillhole (CC1 to CC11) and surface cable extensometer locations (LiDAR hillshade image generated from 2014 BC Hydro survey) (from Woods et al. 2020) 43

Figure 3-3: Seasonal displacement pattern vs. sub-surface temperature fluctuation a) and piezometric level b) 47

Figure 3-4: Hypothesized temperature-driven slope deformation mechanism (from Martin et al. 2011) 52

Figure 3-5: Initial radar antennas a) and new wider field-of-view antennas b) 56

Figure 3-6: Protective Rohacell foam window as viewed from outside shelter a) and inside shelter b) 57

Figure 3-7: Radar signal strength and coverage before a) and after b) installation improvements 58

Figure 3-8: Cumulative apparent average displacements of crest and toe of slope rockface 61

Figure 3-9: Cumulative apparent average and maximum displacements of active zone 65

Figure 3-10: Cumulative apparent average and maximum displacements of active zone 66

Figure 3-11: Seasonal displacement rate of GB-InSAR results vs. extensometer instrumentation data 67

Figure 3-12: GB-InSAR displacement rate maps for separate seasonal periods 68

Figure 3-13: GB-InSAR displacement rate map for entire monitoring period and rockcut surficial features **70**

Figure 3-14: GB-InSAR displacement rate map for data subset from MC5 to 12 and mapped tension crack locations.......... **71**

LIST OF SYMBOLS AND ACRONYMS

mm/y	Millimeters per year
UofA	University of Alberta
BC	British Columbia
GB-InSAR	Ground-based, interferometric, synthetic aperture radar
EM	Electromagnetic
2D	Two-dimensional
1D	One-dimensional
LoS	Line-of-sight
3D	Three-dimensional
DEM	Digital elevation model
USA	United States of America
GHz	Gigahertz
UAV	Unmanned aerial vehicle
TLS	Terrestrial laser scanning
VPN	Virtual private network
Hwy	Highway
ADAS	Automatic data acquisition system
GNSS	Global navigation satellite system
ALS	Airborne laser scanning
W	Watt
V	Volt
A	Ampere
MC	Monitoring Campaign
CAD	Canadian dollars
IP	Internet protocol
C-InSAR	Continuous InSAR
D-InSAR	Discontinuous InSAR
CI	Confidence interval
IQR	Inter quartile range
H:V	Horizontal to vertical
IPI	In-place inclinometer
EDM	Electronic distance measurement
SfM	Structure from Motion image processing
FLAC	Fast lagrangian analysis of continua
UCS	Unconfined uniaxial strength
GSI	Geological strength index
UDEC	Universal distinct element code

1 INTRODUCTION

1.1 Background

Landslides are one of the most widespread and common phenomena among natural hazards and subsequently cause thousands of deaths and injuries and billions of dollars in damages and economic losses, each year, as one of the main sources of loss for life and property worldwide (Kjekstad & Highland 2009; Canuti et al. 2004). These type of events on both natural and engineered slopes pose potential risks to the public, workers, infrastructure, and to the economy as a whole (Macciotta 2013). Specifically, elements of critical importance such as transportation corridors (including highways and railways), mining operations, and dam reservoirs are commonly exposed to such risks. In total, the annual costs associated with landslide hazards for Canada were estimated to reach up to $1.4 billion CAD per year in 2007 (Kjekstad & Highland 2009).

Therefore, in order to address these types of hazards and mitigate their associated risks, engineers, geoscientists, and other earth science specialists can utilize a wide array of tools and technologies (ranging from simple and established to new and complex) to identify, assess, monitor, and gain a greater understanding of landslide processes in the vicinity of human settlement and infrastructure. With the advent of relatively new remote sensing technologies and their application at a variety of different types of sites, it has become of paramount importance to gain an understanding of each technology's benefits, technical limitations, and logistical challenges in order to optimize landslide monitoring systems and schemes based on project objectives.

One such technology used to monitor landslides on both natural and manmade slopes is ground-based interferometric synthetic aperture radar (GB-InSAR). This particular type of monitoring equipment possesses many potential benefits and strengths in comparison, or when used in conjunction to, more traditional, point-wise, in-place geotechnical instrumentation used to monitor slope movement such as slope inclinometers and other remote sensing techniques. These potential benefits include the ability to monitor a large (hundreds of m^2) area, in high density, high temporal frequency, and spatially continuous and highly accurate (down to sub-mm) displacement measurements independent of weather conditions.

Despite these potential benefits associated with this technology, several technical limitations and logistical challenges remain which must be addressed for successful use of GB-InSAR and are discussed at length in the later chapters of this thesis. Many of these limitations and challenges are particularly present in areas that are typical to many Canadian landslide sites which include cold, snowy, mountainous, and heavily vegetated natural slopes. Therefore, this research initiative was established in order to assess the impact of these limitations and challenges, and potential solutions of this technology at such sites.

In September of 2016, a GB-InSAR slope monitoring system, owned by the University of Alberta (UofA)'s Faculty of Civil and Environmental Engineering, was installed across from a known bedrock landslide site referred to as the Checkerboard Creek Rock Slope. With the help of BC Hydro Construction Services and staff from the nearby Revelstoke Dam facility, the system was placed in a timber frame shelter along with accessory power supply and storage equipment, including solar panels and a battery bank.

The Checkerboard Creek Rock Slope site consists of an approximately 2 to 3 million m^3 bedrock landslide with a measured average rate of displacement of 10 mm/y located about 2 km north of the Revelstoke Dam, on the east shore of the Revelstoke Reservoir, about 8km north of the town of Revelstoke, British Columbia (BC). This landslide site and the GB-InSAR equipment location were chosen for multiple reasons. Firstly, BC Hydro, as an owner and operator of multiple large hydroelectric power generation facilities, and responsible for the on-going monitoring of their respective reservoir slopes and known landslide sites, had expressed interest in assessing the applicability of relatively new remote sensing slope monitoring technologies such as GB-InSAR,their ability to provide improved monitoring and site assessment capabilities, evaluation of the challenges of the GB-InSAR regarding data quality and instrument requirements, and the opportunity to obtain improved understanding of a particular landslide on which it was deployed.

The Checkerboard Creek landslide represented one such site with an extensive system of in-place monitoring equipment with a large database of long-term historical instrumentation information that BC Hydro was willing to share with the UofA for GB-InSAR data validation and analysis purposes. In addition, other previously completed research at this site by the UofA had established familiarity with it, its challenges, existing literature, and known landslide deformation mechanisms. Ultimately, this site had several features that made it ideal for this type of slope monitoring, while also posing significant logistical and technical challenges that could assist in the assessment of this technology's applicability at similar sites.

For one, the site had a bare rock cut at the toe of the slope that could provide strong radar wave reflections and signal strength and therefore a higher probability of reliable deformation measurements over time. As well, an established area, about 1.3km west of the rock slope, with existing licenses to place equipment and clear vegetation, was located on the opposite (western) side of the reservoir with a clear view of the entire site. This provided the ideal location for the GB-InSAR equipment, nearly perpendicular to the average landslide direction of movement, with relatively easy access, yet out of the way enough to reduce risk of vandalism and damage to the equipment.

Even so, the site also posed many difficulties with the implementation of the GB-InSAR equipment. While the toe of the slope may have been exposed bedrock, relatively vertical and free of vegetation; the upper portion of the slope was heavily vegetated and at a much lower angle and therefore would significantly reduce the ability of the radar to measure ground surface displacements. In addition, the site consistently experiences significant snowfall over the winter months that could potentially further obscure the radar signal. Finally, this inclement winter weather, in conjunction with no existing electrical power service, short daylight hours at the base of a steep, north-south oriented valley, meant that solar power generation was necessitated but significantly limited. Therefore, alternations were made to the system as part of this research in order to meet the challenges such as this and others related to operating in Canadian site conditions.

1.2 Scope and Objectives

In May of 2018, I was assigned to this project site for the research component for my Master of Science graduate degree. At the time, the GB-InSAR system had collected data over a nearly two-year timespan. However, the collected data was limited to relatively short, discontinuous monitoring campaigns due to solar power generation limitations and other logistical challenges and difficulties. Therefore, in addition to the detailed analysis and assessment of the GB-InSAR data and the equipment's ability to successfully monitor the site, several objectives were established in order to address the power system limitations and other challenges. At this time, a preliminary evaluation of the GB-InSAR data had been completed by Dr. Macciotta and presented at the Geohazards 7 Conference (Macciotta et al. 2018).

Therefore, the objectives for this phase of the research at the site included :

- Define an implementation procedure for GB-InSAR installations in remote mountainous areas by:
    - Resolving the solar power system limitations at the Checkerboard Creek site by increasing the system's power generation and electrical energy storage capacity;
    - install a telecommunications system for remote access to the equipment;
    - improve spatial coverage and radar signal strength in areas of the site that were not currently covered by strong radar signal returns;
- Evaluate the effectiveness of GB-InSAR for remote, slow-moving landslides with limited bared earth exposure and seasonal snow cover by:
    - Determining benefits and limitations of GB-InSAR technology in comparison to other monitoring methodologies at the research site;
    - compete a detailed analysis of the recorded GB-InSAR data, including validation of the GB-InSAR results with in-place instrumentation data;
- Develop an understanding of the surface deformation patterns of a large rock slope within the footprint of a hydroelectric reservoir by:
    - more clearly defining boundaries of the active zone of movement at the site;

- evaluating hypothesized displacement mechanisms and landslide kinematics; and,
- interpreting seasonal displacement pattern by comparing GB-InSAR results to in-place instrumentation data and previously completed numerical modelling

1.3 Methodology

The initial work related to this research at the Checkerboard Creek Rock Slope site primarily focused on:

- Field work associated with upgrading the existing GB-InSAR system and associated equipment (such as power and telecommunications systems);
- data collection and synthesis; and,
- review of the current state of practice on slope monitoring and of existing scientific literature on GB-InSAR technology, other remote-sensing and geotechnical monitoring techniques, and geotechnical assessment and detailed analysis of the identified landslide site and Revelstoke Dam Project

The field work portion of the research first included travelling to site and familiarization with the existing GB-InSAR equipment installation and site features. This included access to the GB-InSAR shelter via a gravel logging road and marked foot path, operation of the solar power generation and battery system along with the gas generator and battery charger, operation of the GB-InSAR equipment itself and use of associated software, and data acquisition to be downloaded for later analysis. Later field work also included site reconnaissance of the landslide site on the opposite side of the reservoir and collection of other field data.

Once this initial field work was complete, work began to address the shortcomings of the existing solar power system to increase the operational timespan of the GB-InSAR equipment, and therefore increase the amount of monitoring data acquired, and reduce the necessity of regular site visits. In parallel to addressing the power system, work began to add telecommunications to the site to facilitate remote access to the GB-InSAR operating software and radar data.

The solar power equipment used was ordered from and supplied by Solar Super Store of Edmonton, AB and installed by BC Hydro Revelstoke field technician staff with collaboration with myself and others from the UofA. Mobile crane equipment was used to lift the equipment from the gravel access road up to the top of the rock bluff where the shelter is located.

Installation of these improvements were not initially successful and required additional field work and site visits. Firstly, the battery bank was initially configured in a way that did not allow for even discharge and recharge of each battery cell. This was resolved by re-wiring each battery cell to a central positive terminal (bus bar) and negative terminal connecting to the electrical load (GB-InSAR equipment) and energy source (solar power controller). Secondly, it also became apparent that with the new 60A solar power controller, in the case of a loss of power due to a lack of sunlight or other restrictions, the controller would also lose power and not restart without intervention by onsite personnel and therefore not charge the batteries further. Therefore, a low voltage disconnect relay was installed between the battery bank and radar equipment that would disconnect the electrical energy load (GB-InSAR) from the batteries in the case of a low voltage condition, allowing for the solar power controller to remain operational and continue to charge the batteries until sufficiently recharged.

The addition of a telecommunications system for remote access consisted a cellular data modem and wireless router which was installed onsite and plugged into the onsite laptop that operated the GB-InSAR system. The weak and inconsistent cell signal at the shelter location was strengthened by the installation of an external directional antenna pointed toward the closest cell tower. Remote access to the laptop and associated software was achieved through widely available VPN, remote desktop, and FTP (file transfer) software. The wireless router also provided the ability to communicate with others while onsite in case of emergency or for assistance with trouble shooting equipment operation issues.

Data relevant to this research was primarily collected from two separate sources and consisted of two different date types. First, both raw and processed GB-InSAR data was collected from the onsite computer and from Dr. Macciotta’s preliminary assessment (Macciotta et al. 2018). This was provided with additional related data including site photos, data processing logs, mask files, and other remote sensing data including terrestrial LiDAR scans and UAV photogrammetry files. Second, historical data from in-place instrumentation including slope inclinometers, extensometers, survey points etc. were collected from BC Hydro along with aerial LiDAR scan data for DEM generation and internal BC Hydro literature and reports regarding the Checkerboard Creek site. Some other data was also collected from nearby Environment Canada weather stations, and from Taylor Piller of Simon Fraser University, another graduate student actively conducting research at the site. All this data was then organized, summarized, and synthesized for the purpose of detailed analysis.

In addition to collection and synthesis of field data from the research site, a detailed literature review was completed on relevant subject matter. A summary of this literature review and its various stages is described in the following section. Upon completion of this literature review, analysis of the GB-InSAR data began. The initial analysis of this data focused on the validation of the GB-InSAR results from the discontinuous monitoring campaigns with that from in-place instrumentation, and assessing the systems capability to successfully monitor slope displacements given the numerous logistical challenges at site and the technical limitations of the GB-InSAR technology, specifically slope vegetation and snow-cover. This analysis was the basis for the first journal paper related to this research which can be read in Chapter 2.

The GB-InSAR data was processed using Persistent Scatterer Interferometry techniques due to limited solar power generation during the initial installation of the monitoring equipment at this site restricted the data to be largely acquired discontinuously (D-InSAR) from October 2016 to March 2019. With D-InSAR, instruments are typically used in multiple separate monitoring campaigns (Monserrat et al. 2014). This same methodology is also used in a similar fashion in satellite based InSAR applications, as it acquires data discontinuously based on the satellite's orbital return period. The processing of D-InSAR data poses substantial technical differences compared to continuous data (Monserrat et al. 2014), however is outside of the scope of this research and is discussed in Crosetto et al 2016. One of the critical issues with D-InSAR data is obtaining a sufficiently high coherence, as large time gaps can lead to severe coherence loss (Monserrat et al. 2014).

For the purposes of this research, IDS Georadar provided their Repeat Pass software, which utilizes the persistent scatterer technique by taking the best matches from temporally disparate monitoring campaigns to output a 2D displacement map for locations within the monitored area within a set coherence threshold. The maps output from IDS's Repeat Pass tool were then aggregated for each monitoring campaign in Esri ArcMap to determine the cumulative displacement. An assumed stable zone to the north of the actively moving area of the slope and where coherence is high was selected and the data corrected to be relative to this area to compensate for potential apparent movement due to snow accumulation and melt in the fall and spring months, respectively. Weather data including recorded precipitation over the monitoring period and onsite photography and notes were also used to analyze the snow conditions at site.

Further analysis of the data collected took a more granular and broader assessment of both the GB-InSAR results and historical instrumentation data in order to develop further insights into numerous aspects of the Checkerboard Creek Rock Slope landslide. These aspects included assessment of the lateral extents of the landslide's active zone of movement, the landslide deformation mechanism, and seasonal displacement pattern. This analysis was the basis for the second journal paper which can be read in Chapter 3.

In order to assess the lateral extents of the active zone of the landslide, the velocities of resulting individual pixels from the displacement map were grouped into ranges of values from inactive/not moving up to more than 10mm/y (the maximum average annual slope velocity based on historical in-place instrumentation data). A minimum velocity threshold of 2mm/y was applied to define the estimated lateral boundary of the active zone due to the apparent accuracy of the results. Analysis of the landslide deformation mechanism was carried out by comparing apparent displacement rates of the crest and toe of the active slope area. If the GB-InSAR monitoring results were to be consistent with previously hypothesized deformation mechanism of rotational toppling, then the displacement rate of the crest of the slope would be expected to be greater than that of the toe of the slope. Assessment of the observed seasonal displacement pattern of the Checkerboard Creek Rock Slope site was conducted by analyzing differences in average seasonal displacement rates of the GB-InSAR results and comparing them to high-frequency in-place instrumentation data such as near-surface extensometers and deeper in-place inclinometers (IPIs). Both these types of instruments indicate a well-defined seasonal displacement pattern, however, differ in timing, with the extensometers indicating accelerations in the late fall during cooling of the ground surface, while the IPIs record accelerations in the spring associated with increased groundwater piezometric levels due to infiltration from rain and snowmelt.

1.4 Literature Review

As stated in the Preface, this is a "paper-format" style dissertation, meaning that Chapters 2 and 3 were written to be submitted as complete journal articles and have either been published or submitted for publication as such. Included in each journal article, and therefore each chapter, is a separate literature review in support of the work presented. However, in addition to these separate literature reviews, this section provides a summary to provided context for this research in terms of state of practice for landslide monitoring and assessment, particularly focussing on remote-sensing techniques and specifically GB-InSAR.

The literature review for the first paper included in Chapter 2 focused primarily on the fundamental theory of GB-InSAR technology, as well it's pros and cons versus different types of slope monitoring methodologies including both more conventional in-place instrumentation and other remote sensing technologies such as satellite-based InSAR, LiDAR, GNSS, and UAV photogrammetry. Also included was the review of literature pertaining to the effect of snow-cover on the efficacy of GB-InSAR monitoring and on details regarding the Checkerboard Creek Rock Slope site including site geology, ground water conditions, instrumentation, and current understanding of landslide deformation.

In contrast, the literature review for the second paper, included in Chapter 3, focused on previously completed numerical slope stability modelling and historical in-place instrumentation data interpretation and how both related to current understanding of slope deformation triggering mechanism(s) and landslide kinematics. Also included was a deeper review of information regarding the development and investigation history of the Checkerboard Creek Rock Slope site.

1.4.1 Landslide Monitoring for Interpretation and Early Warning

Conventional slope monitoring systems such as survey monuments or slope inclinometers utilized pointwise measurements in short-duration, low-frequency campaigns (Crosta et al. 2013). Although useful in understanding landslide behavior, these methods can offer limited capabilities for characterizing landslide behavior, capturing widespread and spatially continuous data, understanding of sensitivity to deformation triggering mechanism(s) and related response time, event duration; and early warning (Crosta et al. 2013). However, recent advances in remote-sensing technologies such as GB-InSAR have some advantages over more traditional means to overcome such limitations (Crosta et al. 2013). These methods can cover a wide area in the scale of several square kms with a map of dense continuous data 24 hrs a day in all weather conditions (Lombardi et al. 2017). The GB-InSAR process can also be automated and as use as operational monitoring tool and can be installed outside the area of risk. Inverse-velocity methodologies pioneered by Fukuzono (1985) can also be applied to provide warning of future slope failure.

Installation of in-place instrumentation such as slope inclinometers and extensometers pose several logistical challenges and potentially significant associated costs. These challenges include gaining access to site for heavy equipment such as a drill rig. As well, both down-hole instrumentation and surveying by total station (whether robotic or otherwise) only provides data for a single point on the ground surface. These difficulties regarding access and drill equipment can mean installation of a single instrument can be in the order of hundreds of thousands of dollars CAD.

However, it should be noted that the primary benefit to this type of slope monitoring when compared to GB-InSAR and other remote sensing technologies is the ability to provide subsurface data with depth which can allow for the identification of failure surfaces and an increased understanding of the landslide failure mechanism. For this reason, GB-InSAR is unable to completely replace all in-place instrumentation for many projects. That being said, it may by able to supplement such monitoring methodologies, reduce the number of total drillholes required, and therefore potentially reduce the overall cost of site assessment and monitoring cost.

1.4.2 Remote-Sensing Techniques for Landslide Monitoring

In recent years, remote-sensing techniques, defined as the science of collection of information about objects or areas from a distance, have gained more widespread use in the field of geohazard monitoring and site assessment. There are a wide range of difference technologies and techniques all with unique advantages and limitations depending upon the application and site characteristics. Outside of GB-InSAR, other typically used remote sensing techniques in the field of geotechnical engineering and geoscience include satellite-based InSAR, LiDAR, UAV Photogrammetry, and GNSS/GPS.

In the case of satellite based InSAR monitoring, due to its large distance from the ground surface, it can cover a much larger area (tens to hundreds of square kms); although has a much lower spatial resolution, with pixel sizes typically in the range of 15 to 30m (Tarchi et al. 2003). Another key limitation is that the data collected is not continuously as the satellite has a set revisiting time dependent upon its orbital period typically ranging from approximately 11 to 46 days. This restriction in temporal resolution limits this technique from being utilized as an operational system for early warning and limits its ability to detect rapid ground movements (Journault 2017).

Similar to GB-InSAR, satellite-based InSAR outputs LoS displacements, however, due to the set orbital path of the satellite, it is impacted by the relative geometry and inclination of the target slope (Colesanti and Wasowski 2006, Wasowski and Bovenga 2014). Ideally, the slope should be in a sub-parallel direction to the LoS. However, in practice the LoS is usually offset from the ground movement in both aspect and inclination; therefore, the InSAR will detect only a portion of total ground movements (Wasowski and Bovenga 2014). In comparison, terrestrial LiDAR or laser scanning (TLS) is another emerging remote sensing method for monitoring slopes (Fey and Wichmann, 2017) which has many advantages including acquisition without access, no measurement point installation, and provides high-resolution spatially continuous data over a large area (Fey and Wichmann, 2017). TLS differs from radar based technology such as satellite and ground-based InSAR by using laser pulses in the infrared spectrum and subsequent detected returns to create a point-cloud of distinct x,y,z coordinates. After acquisition of two equivalent point-clouds of the same site, they can then be overlaid and compared in a technique known as change detection which can identify and quantify areas of deformation (Hutchinson et al. 2015). TLS also has a higher resolution in comparison to GB-InSAR with multiple points per square meter, whereas GB-InSAR is typically restricted to a minimum resolution of 0.75m due to the radar's wavelength (Ku band for most widely available equipment).

UAVs in conjunction with the use of structure-from-motion (SfM) image processing have become common-place as a reliable low-cost, solution for geotechnical monitoring purposes (Peppa et al. 2018). Processing of photos captured from cameras mounted on UAV's using SfM can be used to automatically generate dense point clouds similar to those from LiDAR/TLS (Snavely et al. 2008; Remondino et al. 2014) and be compared using the same change detection techniques to identify areas of movement and calculate displacements between surveys. Although GB-InSAR and TLS offers higher spatial resolution, they require much higher financial investment (Travelletti et al., 2012).As well, TLS and GB-InSAR require to be installed at a static/fixed site and therefore occlusions or shadows can occur due to the oblique angle of the radar waves and laser pulses. This limitation can therefore necessitate numerous scanning positions (Jaboyedoff et al., 2012, Severin et al. 2014), increasing operational cost. In juxtaposition to this, UAV's can freely fly over any given site providing numerous different viewing angles which limit the presence of occlusions in the created point cloud.

The accuracy of UAV photogrammetry for geotechnical monitoring purposes largely depends generally on the resolution of the photo sensor used, the nature of the ground cover (vegetation), and the SfM image processing methodology used (such as the inclusion of ground control points (GCPs) or post processing kinematics (PPK) which can achieve accuracies as little as a few centimeters).

Devices that utilize GNSS/GPS systems are restricted to recording deformation data of a single data point per device and also require access to the site for installation. However, it does have many of the same advantages as GB-InSAR, including high frequency measurements possible during the day or night and under bad weather conditions (Pecoraro et al. 2018). Current equipment can detect slow landslide movements down to a rate as little as 1–2 mm/year within a period as short as 3 years (Wang et al. 2014). Compared with conventional monitoring techniques, this typically increases survey accuracy, productivity, monitoring capability, and reduces cost (Wang et al. 2015).

1.4.3 Perceived Limitations of GB-InSAR Monitoring

Since their development and initial application, both satellite and ground-based deployments of InSAR technology have seen use on a progressively wider array of subject sites and purposes. Nonetheless, applications of this technology at landslide sites outside the mining industry have been primarily focused on landslides in Europe (Barla et al. 2011; Corsini et al. 2006; Frodella et al. 2017; Lombardi et al. 2017; Matteo et al. 2017) with limited adoption in Canada (Dehls et al. 2010) and some in Colorado (Gomez et al. 2019; Rosenbald et al. 2013; Schulz et al. 2011). This apparent lack of adoption might be due to a variety of factors including: the relatively high cost of the instrumentation (Scaioni et al. 2018), the general unfamiliarity of professionals with the technology, and perceived limitations and logistical. These factors directly relate as to why GB-InSAR has been most widely used at mining sites, as they typically have flat, bare-ground surfaces that which provide strong radar reflections and operators with sufficient resources to purchase or rent such equipment.

As well, a key limitation of all radar systems, including GB-InSAR is that they are restricted to providing only apparent 1D LoS displacements, in the direction from the target, either towards or away from the scanner. In addition, whatever the subject target may be, a strong and consistent enough reflection of the radar waves must be established to accurately track movements over time. As such, the most significant source of noise and monitoring inaccuracies is the presence of vegetation; Snow cover can also affect the ability of GB-InSAR to reliably monitor movements (Dehls et al. 2010) deespite its apparent ability to penetrate the snow surface. This can result in lower temporal coherence and potentially an inability to provide useful results in winter months (e.g., Dehls et al. 2010; Carlà et al. 2019).

GB-InSAR equipment is relatively mobile and can easily be installed in a small trailer, shelter, or left uncovered. However, the equipment is not as easily transportable in comparison to TLS or UAV equipment, which can be usually be carried by a single person without considerable effort. Meanwhile, GB-InSAR systems are comprised of several, relatively large and heavy components. As well, a lack of access to a reliable power source can increase costs and decrease the reliability and mobility of GB-InSAR systems. This poses a significant challenge for remote and mountainous sites. Deep and steep-sided mountainous valleys with limited sunlight, frequent overcast and inclement weather, and heavy precipitation in the form of snow can significantly decrease the amount of electricity that can be generated by solar power systems, especially during winter months.

2 PAPER 1: GB-InSAR monitoring of vegetated and snow-covered slopes in remote mountainous environments

This chapter was published as *GB-InSAR monitoring of vegetated and snow-covered slopes in remote mountainous environments*. (Woods et al. 2020) in the Journal of the International Consortium on Landslides and published online on May 4th, 2020 (DOI 10.1007/s10346-020-01408-4.

2.1 Introduction

As a member of the International Consortium on Landslides, the University of Alberta is actively working to improve technologies for the monitoring of natural hazards as part of the Kyoto 2020 commitment for global promotion of understanding and reducing landslide disaster risk. GB-InSAR has been successfully implemented for near real-time monitoring of natural and man-made slopes (Atenzi et al. 2014, Barla et al. 2015, Dick et al. 2015, Tarchi et al. 2005) and, as such, should be of interest to a wide audience in areas where ground displacements put people and property at risk. This includes individuals and organizations such as geotechnical engineers, consultants, contractors, governmental bodies, and civil infrastructure operators including railways, highways, and utilities (hydroelectric dams, reservoirs, and pipelines). However, despite this, GB-InSAR has seen limited use in Canada outside of the mining industry. This lack of adoption has been attributed to difficulties associated with providing continuous power at what are predominantly remote locations as well as caveats that snow may impact the quality of results (Carlà et al. 2019; Dehls et al. 2010), which leads to concerns that these expensive installations may not work in all conditions.

This paper presents the results of a project to install a GB-InSAR system to monitor a 2 to 3 million m^3 bedrock landslide with a measured average rate of displacement of ~10 mm/y (Martin et al. 2011; Watson et al. 2007). This includes an examination of the advantages, limitations, and challenges associated with GB-InSAR for monitoring ground movements in remote northern conditions. The selected site is characterized by long periods of deep snow cover, cold temperatures, no connection to the electrical grid, and a location within a steep valley that limits hours of daylight for solar power. This paper also provides details of the solutions developed for the successful operation of the GB-InSAR equipment at this site, and a validation of the results through a comparison with existing geotechnical instrumentation. The novelty of this paper is that these results have been applied at a site that has many of the same challenges that are applicable to all northern (cold) climates and mountainous environments, where monitoring is required in remote areas.

2.2 Ground-based InSAR

2.2.1 Fundamentals and Applications

GB-InSAR is a microwave frequency radar system that can transmit and receive electrocmagnetic (EM) signals and arrange them in a two-dimensional (2D) image map of instrument to target one-dimensional line-of-sight (1D LoS) distances (Lombardi et al. 2017), independent of sun illumination or weather conditions. Two image maps of the same area from scans taken at different times can then be used to generate interferograms, i.e., phase difference images (Burgmann 2000; Wasowski and Bovegna 2014). These interferometric images can be presented in three dimensions (3D) by overlaying them on a digital elevation model (DEM) (Atzeni et al. 2014). Further details about the technology and processing methodologies can be found in Pieraccini and Miccinesi (2019), Monserrat et al. (2013), Corsini et al. (2007), Colesanti and Wasowski (2006), Ferretti et al. (2007), and Burgmann et al. (2000).

GB-InSAR has some advantages over traditional monitoring (Crosta et al. 2013) and can be complementary when used in tandem with other techniques (Barla and Antolini 2015, Carlà et al. 2018). Some of the advantages, summarized by Monserrat el al. (2014), include the ability to monitor a wide range of deformation rates (from a few mm/y to m/y) and very high precision (sub-mm to a few mm depending on the target's distance and geometric characteristics) (Table 2-1). In comparison, a key limitation of satellite InSAR is that the data are not continuous as each satellite has a set revisiting time based on its orbital period. In addition, GB-InSAR monitors relatively smaller areas than satellite-based systems (on the scale of 1-2 km^2; Monserrat et al. 2014) and provides a map of dense continuous data 24 hours a day in all weather conditions (Lombardi et al. 2017).

Table 2-1: Monitoring Technique Summary

Monitoring Technique	Accuracy	Temporal Resolution	Spatial Resolution	Range	Density
GB-InSAR*	≤ mm	< 3 min	Continuous, 10,000s of pixels	≤ 5 km	High
RAR*	≤ mm	5-30 min	Continuous, 100s of pixels	≤ 2.5 km	Medium to High
Satellite InSAR†	cm	11-46 d	Continues, millions of pixels	Unlimited	Low
LiDAR / Laser Scanning*	≤ cm	min to h	Continuous, millions of points	≤ 3 km	Very High
Robotic Total Station*	mm	10s of min	Pointwise	≤ 1km	Pointwise
UAV Photogrammetry‡	cm	min to h	Continuous, 1000s of points	≤ 1km	Medium to High
GNSS*	≤ cm	min	Pointwise	10s of km	Pointwise

*Atzeni et al. (2014)
† Ferretti et al. (2007)
‡ Fey and Wichmann (2016)

In Canada, GB-InSAR has been mostly used in the mining industry for monitoring open pit mine slopes (Carlà et al. 2018; Dick et al. 2014; Severin et al. 2014). In other regions, it has also seen extensive use on natural slopes since its first application in the Italian Alps (Tarchi et al. 2003). GB-InSAR is also being used for less typical applications, including monitoring movements of rockfall (Matteo et al. 2017), sinkholes (Intrieri et al. 2013), glaciers (Noferini et al. 2009; Whitehead et al. 2010), structures (Tarchi et al. 1999), and volcanoes (Spaans and Hooper 2016). Since their introduction, both satellite-based and GB-InSAR have seen progressively wider applications. However, application on landslide sites outside the mining industry have been focused on sites in Europe (Barla et al. 2011; Corsini et al. 2006; Frodella et al. 2017; Lombardi et al. 2017; Matteo et al. 2017) with limited adoption in Canada (the exception is monitoring of the Turtle Mountain/ Frank Slide; Dehls et al. 2010) and multiple sites in Colorado, USA (Gomez et al. 2019; Rosenbald et al. 2013; Schulz et al. 2011). This lack of widespread adoption may be due to a variety of factors, among which is the relatively high cost of the instrumentation (Scaioni et al. 2018), the general unfamiliarity of Canadian engineers and geoscientists with the equipment and data obtained, and perceived limitations and logistical challenges associated with the technology. These factors relate to why GB-InSAR has been mostly applied on mining projects is as it is most effective on flat, bare-ground surfaces that are typical of mine slopes that require long-term continuous monitoring. However, this significantly limits its applicability to natural slopes in Canada that commonly feature dense vegetation and snow cover in the winter months.

2.2.2 Limitations and Logistical Challenges

A key limitation of all radar systems is that they only provide 1D LoS displacements in the direction from the target toward or away from the scanner. This means that real 3D displacement information on kinematics may be missed (Severin et al. 2014). As well, shadows or occlusions occurring within the study area can lead to some displacements not to be detected (Carlà et al. 2018). This may be overcome by simultaneous deployment of two GB-InSAR systems (Severin et al. 2014) or used in tandem with other monitoring technologies such as satellite InSAR (Carlà et al. 2018).

In general, coherence is the quality of two sequential SAR images being compared to determine displacement of an area within the target site and reflects the ability of the target to be measurable through time (Wasowski and Bovegna 2014). Coherence depends on a variety of factors including the physical and geometric characteristics of the measured surfaces and their changes between GB-InSAR images. Higher coherence is achieved when noise in the images from sources such as atmospheric effects is low (Ferretti et al. 2007).

Depending on the site, the ground surface of an area prone to hazards can be highly variable from low angle, highly vegetated soil slopes to near vertical, highly angular rock slopes or cliffs. For GB-InSAR, the most optimal measurements are acquired from large, flat, hard surfaces (e.g., vertical excavated slopes) that are perpendicular to the LoS of the scanner. One of the most significant sources of noise, and therefore lack of coherence is the presence of vegetation. This poses a significant limitation to its applicability to natural landslide sites, which commonly have dense vegetation cover. Snow cover on the ground surface can also obscure movements. Snow is a complex material consisting of a mixture of air, ice crystals, and, at times, liquid water, which complicates interactions with the EM waves transmitted and received by GB-InSAR. The primary sources of backscattering (reflection) from a snow-covered slope include surface scattering at the air-snow interface, ground-snow interface, snow layer interfaces, and volume scattering within the snowpack (Luzi et al. 2010). If high coherence can be obtained from a snow-covered surface, the accumulation, melt, and consolidation of the snowpack may result in apparent movements that are not reflective of the real movement of the ground surface.

The microwave frequency typically used in GB-InSAR (Ku-band: 17.05-17.35 GHz) is more sensitive to the presence of snow and has a smaller penetration depth (approximately 3-4 m in dry snow) when compared to lower frequency radar waves in the C- or S-bands (Rott et al. 2009) used by some satellite InSAR systems. Despite the GB-InSAR's apparent ability to penetrate the snow surface and obtain backscatters from the ground surface, snow can result in lower coherence and potentially an inability to provide useful results in winter months (e.g., Dehls et al. 2010; Carlà et al. 2019).

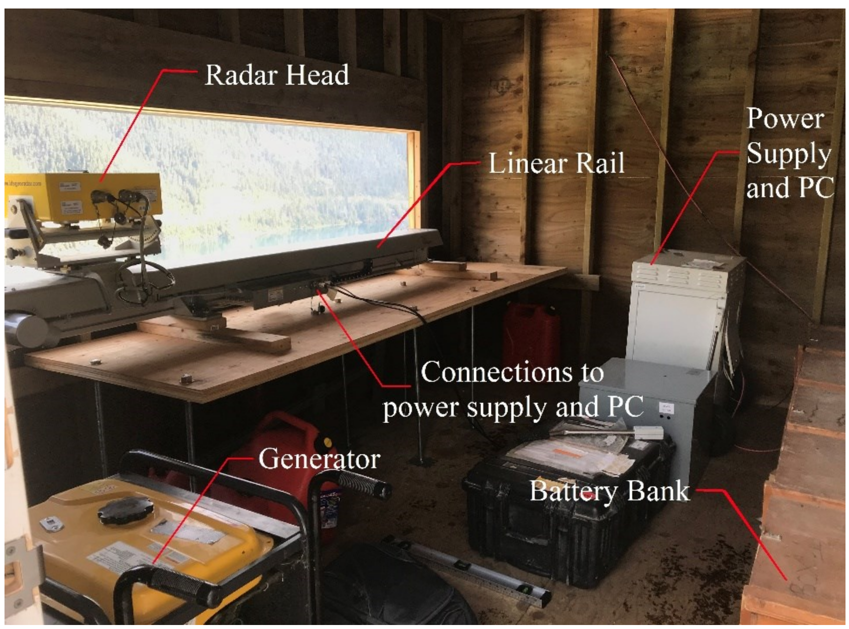

Figure 2-1: GB-InSAR components as at Checkerboard Creek Rock Slope installation (photograph taken by A.Woods, May 2018).

Landslide sites both globally and in Canada can also pose significant challenges regarding access due to remoteness and steep terrain (Carlà et al. 2019), and this may influence the suitability and associated costs with different types of geotechnical monitoring equipment. In the case of GB-InSAR, the equipment is generally mobile and can be installed in a small trailer, shelter, or in some cases left uncovered. However, the equipment is not as easily transported as terrestrial laser scanners (TLSs) or unmanned aerial vehicles (UAVs), which can be carried by a single person without considerable effort; rather, GB-InSAR consists of several relatively large and heavy components (i.e., radar head, linear scanner rail, power supply, a weatherized laptop, connecting cables, and associated power supply and telecommunications equipment; Figure 2-1) that may require several people to transport.

Installing telecommunications equipment with a GB-InSAR system has the benefit of allowing remote connectivity to the monitoring equipment, software, and data. This drastically reduces the need for site visits and related time and costs. Data can be easily transmitted automatically via virtual private network (VPN) and processed by an offsite computer set up to allow for early warning if accelerated displacements are detected. However, many remote areas in Canada have limited to no cellular data reception to permit wireless internet access. A lack of a reliable power source can increase costs and decrease the reliability and mobility of GB-InSAR systems and pose a significant challenge for mountainous sites. Deep and steep mountainous valleys, limited sunlight hours, overcast weather, and precipitation in the form of snow can also significantly decrease the opportunity for solar power generation, especially during winter months. These factors increase the cost and amount of equipment needed to continuously power the system or require alternative power systems to be considered. In addition, cold temperatures decrease the charge capacity of batteries used to store electrical power and run the equipment overnight if solar power generation is used.

2.2.3 Available Solutions

Despite these limitations and challenges, cost-effective solutions are available related to the use of GB-InSAR. Severin et al. (2014) demonstrate that 3D displacements can be determined using two or more GB-InSAR units, but this involves significant additional costs. The most cost-effective solution is installation directly opposite the approximate direction of movement.

The most effective way to address low coherence in areas of vegetation is to install radar corner reflectors. These typically consist of s a three-sided steel pyramid (trihedral) arrangement with the open end directed toward the radar scanner, allowing for strong backscatter reflections (Figure 2-2). These reflectors come in a variety of different sizes depending on the transmission frequency of the radar used; however, typical side dimensions in the 20-25 cm range are often used for ground-based deployments in the Ku-band. These reflectors can be mounted directly on a rock face or elevated above the ground surface on a post or tripod mount (Figure 2-2). Corner point reflectors can also be installed in areas of snow cover by mounting the reflectors above the snowpack. However, installation of reflectors requires access to site, and only provides point-wise data and adds additional costs. Corner point reflectors have yet to be installed at the subject site of this paper, however, are planned to be installed in the upper vegetated area at a later date. Also, at this site, an assumed stable area within the study area is used to compensate for the apparent movement related to snow accumulation and melt on an actively moving zone.

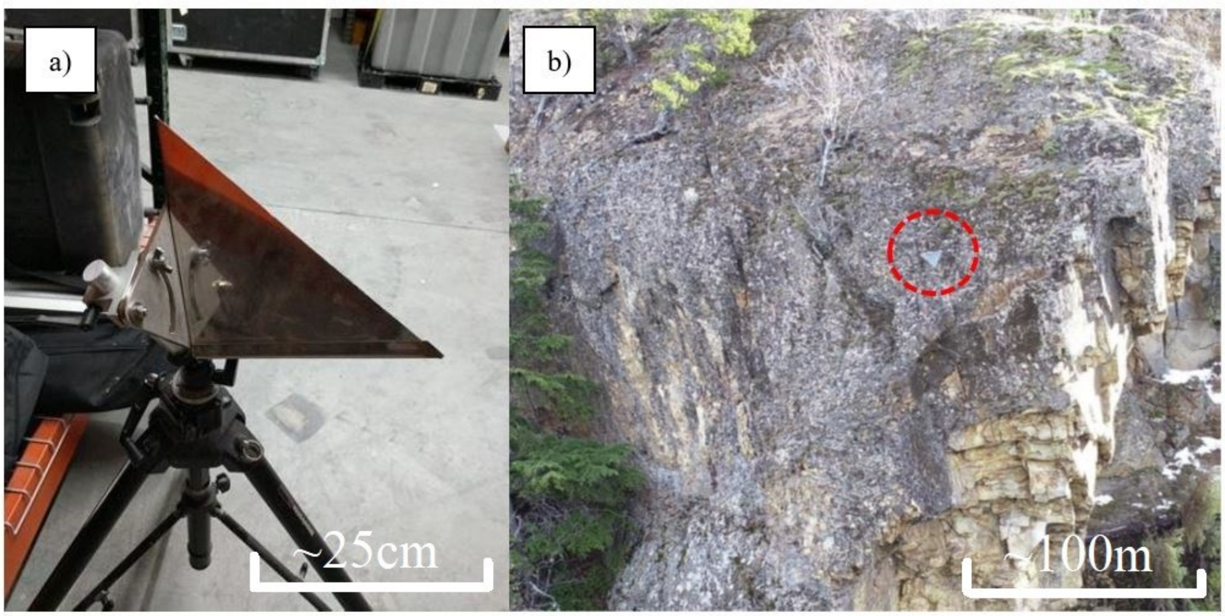

Figure 2-2: Radar corner point reflector on tripod mount (a) and mounted on rock face (b) (photograph courtesy of IDS Georadar)

In areas with limited or no cellular data reception, several options range in cost and installation effort including external directional antennas, cellular signal boosters, and satellite communication links. Where connection to the electrical grid is unavailable, the most common source of electricity for GB-InSAR is either photovoltaic solar panels or small gas generators attached to a battery bank. Generators, however, require regular maintenance and fuel deliveries whereas solar power systems can operate passively with little requirement for regular site visits. In areas of little sunlight, additional solar cells and batteries can be added upon to provide adequate power. Less common remote sources of energy include wind turbines and propane fuel cells.

2.3 Addressing the Challenges of GB-InSAR at the Checkerboard Creek Rock Slope

The Checkerboard Creek Rock Slope was selected as a study site because it possesses many of the attributes that make applying remote sensing technology at many Canadian sites difficult: steep mountainous terrain, amount of precipitation (snow), number of overcast days in the year, and dense vegetation cover. In addition, the exposure rock face at the toe of the slope permitted good radar signal returns, and the wide variety and spatial coverage of in-place geotechnical instrumentation allowed for validation of the GB-InSAR results.

2.3.1 Site Description

The Checkerboard Creek Rock Slope is located approximately 2 km north of the Revelstoke Dam on the Columbia River along Highway (Hwy) 23 and on the east shore of the Revelstoke Reservoir (Figure 2-3). The elevation at the toe of the slope at Hwy 23 is 260 m and 590 m at its crest. It is bounded on the eastern uphill side of the slope by Checkerboard Creek (Figure 2-4), to the south by the lower reaches of Checkerboard Creek, to the north by Ballpark Creek (intermittent flow), and to the west by the Revelstoke Reservoir. It is approximately 600 m wide with an overall slope angle of 30°; however, it is steeper at the toe (45°) near the rock cut excavated for Hwy 23 and flatter in the upper area (25°) (Watson et al. 2004).

The area of active movement of the slide has been interpreted from the site geology, slope topography, and deformation patterns (Macciotta et al. 2016). This area is located towards the central lower portion of the rock slope and is approximately 200 m wide along the direction of Hwy 23 and 150 m deep from the highway to the uppermost tension cracks that define the upper boundary of the deformation area (Figure 2-4). However, the lateral and toe boundaries are less well defined. The active zone of deformation has an average slope angle of 45°, and deformations have been detected down to 50-60 m deep within a zone of higher weathering and lower quality rock masses (Watson et al. 2004). The total volume of this active zone is estimated somewhere between 2 and 3 million m^3.

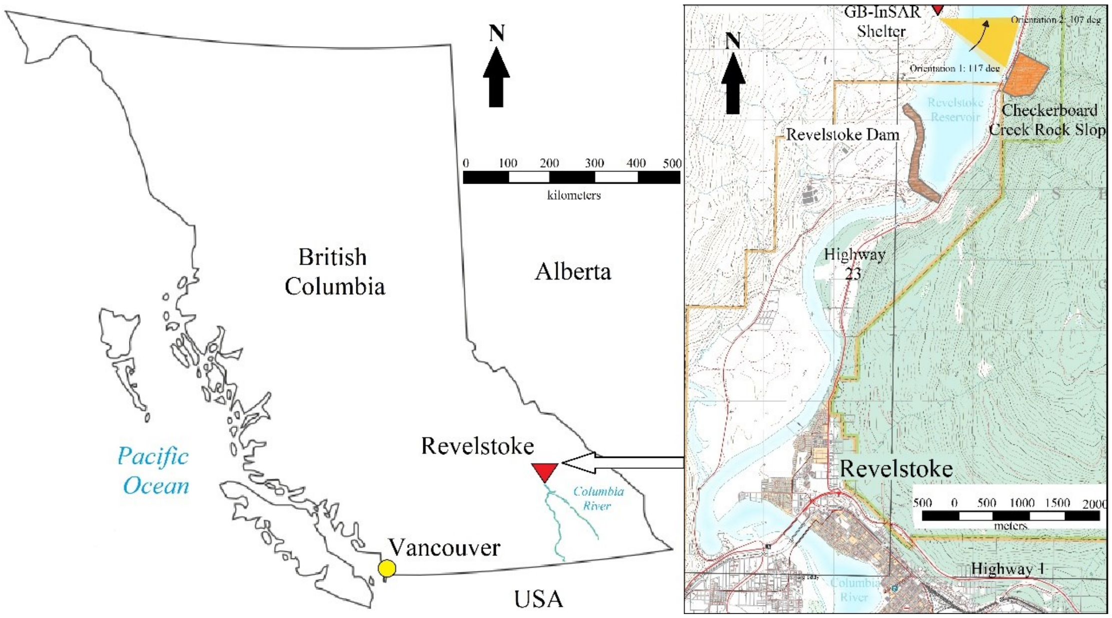

Figure 2-3: Location of the Checkerboard Creek Rock Slope and GB-InSAR installation.

The site geology primarily consists of massive to weakly foliated granodiorite overlying the easterly dipping gneiss and schist of Columbia River Fault, which has developed a broad, regional, brittle deformation zone of altered and mechanically deformed rock (Lane 1984). Rock mass quality ranges from very strong, fresh, undisturbed, and blocky to highly weathered and altered, weak, and disturbed (Macciotta et al. 2018). Discontinuities within the slope have primarily been identified as steeply dipping inward and out-of-slope dipping shears and joints at 60 to 90° from horizontal. There is no evidence of a downslope dipping base of sliding (Watson et al. 2006). Open tension cracks (discrete, planar to sinuous bedrock cracks within outcrops, or collapse features with thin surficial deposit cover) are exposed in the central slope area and trend sub-parallel to the slope contours between an approximate elevation of 650 and 740 m (Macciotta et al. 2016).

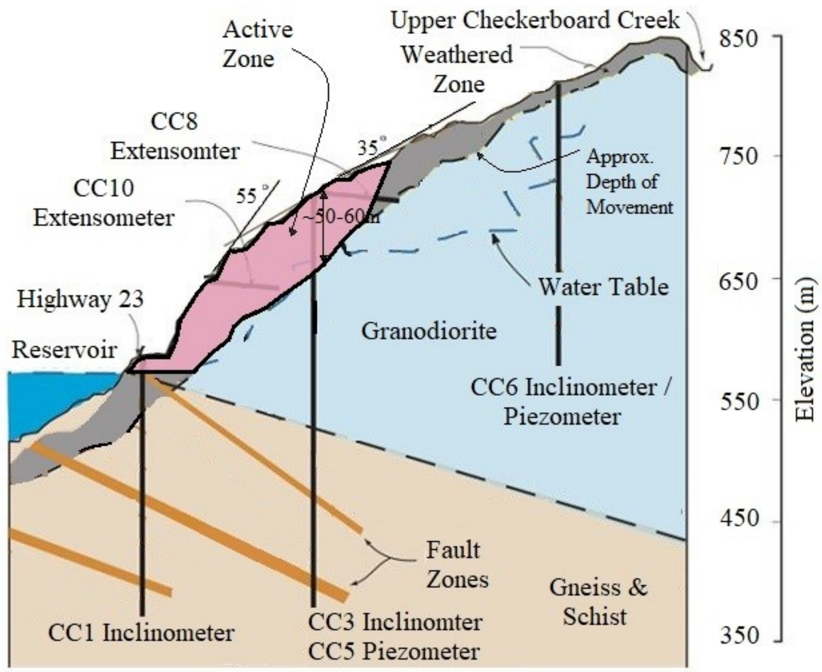

Figure 2-4: Typical geological cross-section of Checkerboard Creek Rock Slope and related in-place instrumentation (after Watson et al. 2006).

Groundwater levels in the slope have been inferred from observations during drilling, site inspections, packer testing, and monitoring of multiple piezometers. These revealed a complex "compartmentalized" groundwater system with saturated conditions at a depth of 50 to 80 m below the slope surface (below the base of the active slope deformation) and with seasonal variations in piezometric levels of up to 20 m (Stewart and Moore 2002). Generally, the piezometric data suggest that a downward pressure gradient exists, with the main source of recharge occurring from infiltration (Watson et al. 2006).

Instruments near the exposed rock face indicate persistent annual seasonal patterns, with accelerated displacements in the early fall to late winter and reduced displacement in the spring and summer (Stewart and Moore 2002; Watson et al. 2004, 2006) as shown in the CC10 extensometer data, Figure 2-9. However, instrument trends further back in the landslide and at depth have a steadier displacement. Interpretation of this displacement pattern shows an accelerated phase during spring snowmelt, when piezometric pressures are at seasonal maximums; investigations regarding the cause(s) of the acceleration are ongoing. The displacement rate is 0.5 mm/y at the boundaries of the active area and up to 15 mm/y within the most active area. These rates are greatest at the surface and decrease progressively with depth.

The deformations are generally widely distributed within the deforming mass but zones where these are more concentrated or absent also exist. These patterns indicate deformations may be due to dilation of the rock mass with discrete block sliding and rotation occurring throughout the mass (Stewart and Moore 2002; Watson et al. 2004, 2006) rather than sliding as a single cohesive block along a failure plane or simple toppling (Macciotta et al. 2016). Geomorphic evidence such as tension cracks indicates a long history of surface displacement of up to 10 m or more (Watson et al. 2006).

2.3.2 Instrumentation and Other Monitoring

An extensive amount of in-place slope instrumentation exists at this site, most installed between 1984 and 2000 (Watson et al. 2006). The locations of some of these instruments are shown in Figure 2-5 and a detailed summary is provided in Table 2-2. The instrumentation includes surface survey monuments (read annually), manual slope inclinometers (annually) and in-place probes (every 6 h), nested standpipe piezometers, multipoint borehole extensometers (every 4 h), surface cable extensometers (annually), strain meters, borehole and surface thermistors, and a weather station that records daily temperature and precipitation values (Macciotta et al. 2016). Annual precipitation at the site is typically between 1500 to 2000 mm, approximately 40% of which occurs between October and January, predominantly as snow (see Figure 2-12 for accumulated snowfall over monitoring period). Air temperatures typically range between −25 and 35 °C, with freezing temperatures prevailing from late November through March. Because the slope is heavily treed, snow depths are highly variable but typically range from 1 to 2 m in mid-winter (Watson et al. 2004). The fall and winter days at the site feature short periods of direct sunlight, frequent overcast weather, and snowfall events between December and March.

Table 2-2: Instrumentation Summary

Instrumentation Type	# Boreholes / Locations	Temporal Resolution
Slope Inclinometer*	5 boreholes (CC1, 3, 4, 6, 7) 180 to 300 m depth	Semi-annual profiles
In-place Inclinometer*	2 boreholes (CC3 and CC4) 7 probes total, 5 operational 33 to 49 m depth	Continuous (max 6 h)
Multi-point Extensometer*	2 boreholes (CC8 and CC10) 12 total, 6 each, 6 to 18m spacing 7 to 60m depth, horizontal	Continuous (max 4 h)
Surface Cable Extensometer	6 measuring 10-30 m zones	Monthly readings excluding December to March
Surface Strainmeter	3 total, aligned orthogonally across steep fault (Meadow Fault)	Continuous
GNSS Sensors	4 sensors	Continuous (noisy with data gaps)
Nested Standpipe Piezometer[‡]	1 borehole (CC2), 3 zones 180 m depth	Manual readings
Westbay Multiport Piezometers	7 boreholes 50 to 300 m depth	14 zones continuously monitored, 50 read manually
Surface and Borehole Thermistors	26 borehole thermistors in 6 boreholes, 1 shallow trench	Continuous
Electronic Distance Measurement (EDM) Surveys[‡]	1 base station, 35 prisms 14 prisms in active zone	Semi-annual surveys

* Time between measurements increases if acceleration detected
[†] Vibrating wire piezometers installed in standpipes
[‡] Some prisms have become damaged by snow or not visible due to vegetation over time

Many of the instruments have been incorporated into an automatic data acquisition system (ADAS) that is continuously monitored at Revelstoke Dam. The current displacement rate only exceeds the measurement sensitivity of the inclinometers after about 6 months as the annual displacement rates are very small and distributed over wide areas within the deforming rock mass (Watson et al. 2006). This further reinforces the need for a highly accurate monitoring system that can cover a large area. Other types of remote sensing at this site include a global navigation satellite system (GNSS) network with four sensors located at different locations around the site and a laser distance sensor. Airborne laser scanning (ALS) was also carried out by BC Hydro in September 2014 and was used to generate the hillshade map and DEM for this analysis.

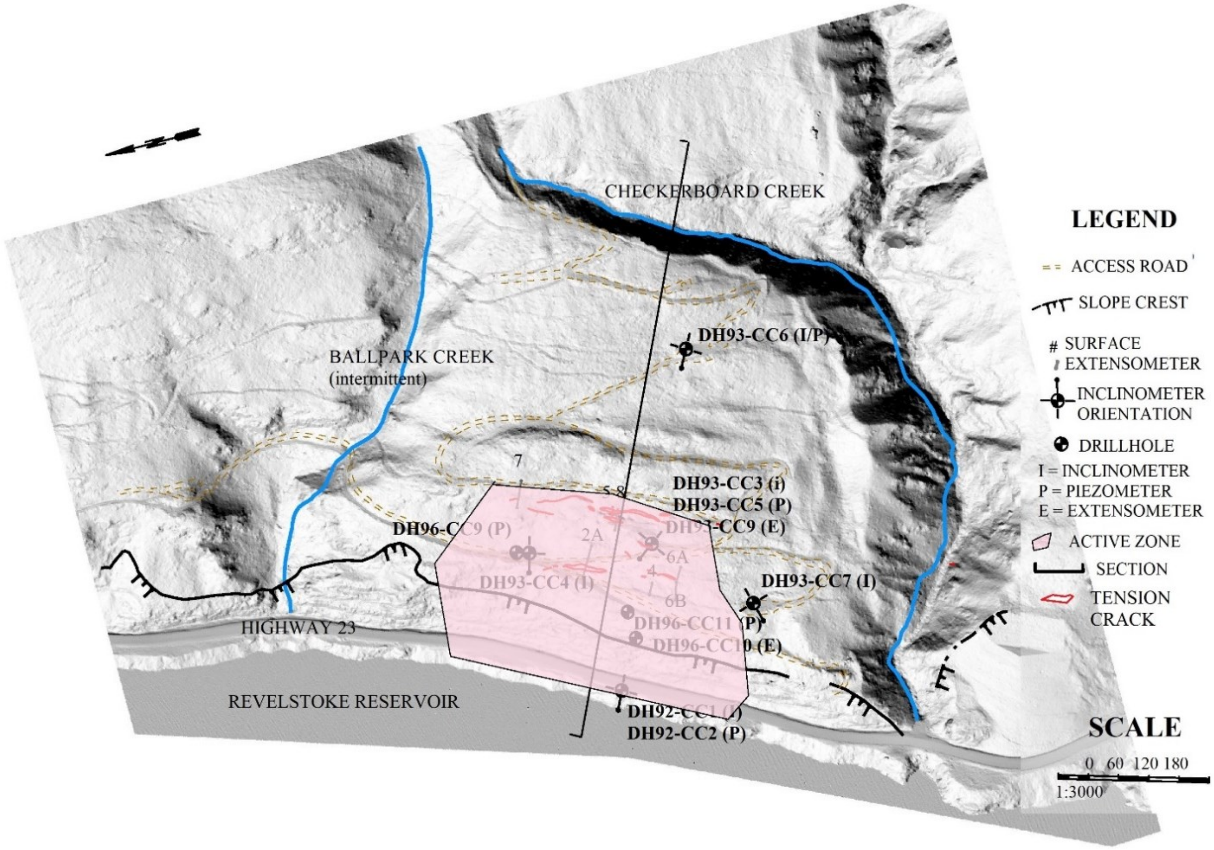

Figure 2-5: Drillhole (CC1 to CC11) and surface cable extensometer locations (LiDAR hillshade image generated from 2014 BC Hydro survey).

2.3.3 Checkerboard Creek GB-InSAR Installation

A model IBIS-L GB-InSAR system manufactured by IDS Georadar was installed in October 2016 on the west bank of the Revelstoke Reservoir and directed toward the Checkerboard Creek Rock Slope, located on the opposite side. The instrument was installed inside a small timber-frame shelter to protect it from weather and wildlife. Initially, the radar transmitted through an open space in the side of the shelter and was directed toward the center of the slide. A transparent protective plexiglass window was later installed in November 2016; this required the radar to be re-oriented slightly toward the north side of the slope due to the overall orientation of the shelter structure and the requirement of the radar to be perpendicular to the window to reduce reflection of the radar waves.

The challenges at the site associated with its climate included the limited availability of sunlight for solar power generation and frequent snowfall in the winter that partially covers the rock face of the slope. The GB-InSAR was initially powered by a solar power system that consisted of a pair of 260 W panels connected in parallel with three 24 V, 100 A, parallel battery packs (Figure 2-6). The system allowed for 5 to 15 d of monitoring during the fall and winter months, resulting in discontinuous data acquisition from October 2016 to March 2019 (1- to 2-week monitoring campaigns (MCs) conducted every 1 to 2 months). A small gas-powered generator was used intermittently to boost and recharge the battery banks. Overall, these challenges translated to limited periods of continuous monitoring and uncertainty regarding slope measurements during the winter months due to atmospheric effects and transient snow cover.

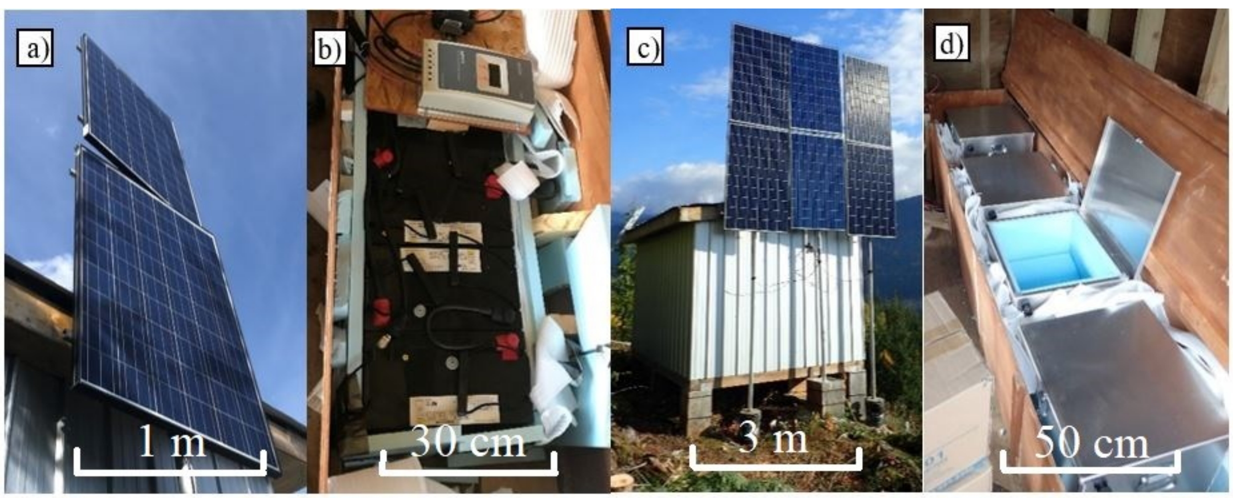

Figure 2-6: Original solar panel installation Oct. 2016 to Oct. 2018 (a) and battery pack and 20 A charge controller (b). Upgraded solar installation Oct. 2018 to present (c) and insulated aluminum battery boxes (d).

The short-term, discontinuous nature of the acquired data over this period negated some of the primary advantages of the GB-InSAR system. Therefore, the solar power system was upgraded in October 2019 by installing an additional four 270 W panels and replacing and upgrading the battery capacity with four new 24 V, 100 A battery packs in insulated aluminum battery boxes (Figure 2-7). Due to the increased power generation from the additional panels, the charge controller was also upgraded from a 20 to 60 A input unit. This upgraded system operated continuously from March to June 2019 and is accessible remotely through VPN. A detailed cost breakdown of the final installation is provided in Table 2-3; however, the most significant cost of any GB-InSAR installation is the radar system itself and software license, which can total close to $400,000 CAD. Rental of GB-InSAR equipment complete with all necessary power, telecom, and shelter equipment is also available at significantly lower rates (approximately $10,000-$30,000 CAD for one to two months). An external directional antenna and an associated power supply connected to the batteries was installed to allow for remote connectivity to the GB-InSAR, with telecom equipment that consisted of a cellular modem with a static IP address.

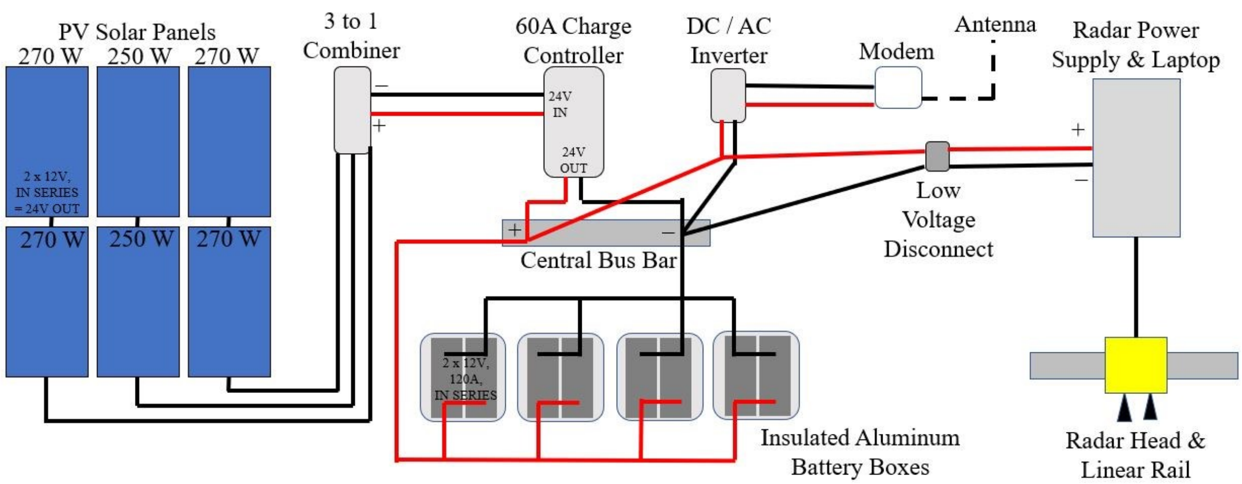

Figure 2-7: Checkerboard Creek GB-InSAR detailed solar power system and telecommunications schematic

Table 2-3: GB-InSAR accessory cost breakdown

Equipment	Unit Price ($CAD)	Total ($CAD)
270 W Solar Panel	260	1560
12V DC Batteries	270	2160
60 A Charger Controller	660	660
3 Panel Combiner	105	105
Cell Modem	270	270
External Outdoor Antenna	125	125
Misc. (Cables, breakers etc.)	n/a	830
TOTAL	n/a	5710*

* Does not include cost for materials, construction, and installation of shelter or battery boxes, which were provided by BC Hydro

2.4 Data Processing and Validation

2.4.1 Data Collection

GB-InSAR data can be acquired using two different acquisition modes: continuous (C-InSAR) and discontinuous (D-InSAR) (Monserrat et al. 2014). In C-InSAR, the instrument is left installed onsite to continuously acquire data on a regular basis, typically every 3 to 15 min (Monserrat et al. 2014), allowing for "near real-time" monitoring of a site (Tarchi et al. 2005). This methodology is appropriate to measure relatively fast deformation phenomena (mm/d to m/d), providing a monitoring tool that can support the management of emergency scenarios (Casagli et al. 2003; Tarchi et al. 2003, 2005). For slower phenomena (mm/y) such as the Checkerboard Creek Rock Slope, the GB-InSAR equipment must be installed onsite long-term or discontinuous methodologies can be applied. Due to the solar power generation restrictions during the initial installation of the GB-InSAR at this site, most data were acquired discontinuously (October 2016 to March 2019); this paper therefore discusses the results and analysis of these datasets.

With D-InSAR, instruments are typically used in several campaigns, revisiting a given site periodically (Monserrat et al. 2014). This same methodology is also applicable for satellite based InSAR, which acquires data discontinuously based on the satellite's orbital return period. The processing and analysis of D-InSAR data poses substantial technical differences compared to C-InSAR data (Monserrat et al. 2014). One of the critical issues with D-InSAR data is obtaining a sufficiently high coherence, as large time gaps can lead to severe coherence loss (Monserrat et al. 2014).

For this installation the Checkerboard Creek site, IDS Georadar provided their Repeat Pass software, which takes the best matches from subsequent monitoring campaigns to output a 2D displacement map for locations in the monitored area within a set coherence threshold. This uses a proprietary algorithm adopting the same processing methodologies applied to satellite InSAR techniques. The maps output from IDS's Repeat Pass tool can then be aggregated for each monitoring campaign in Esri ArcMap to determine the cumulative displacement. An assumed stable zone to the north of the slide (see Figure 2-8) where data coherence is high was then selected and the data corrected to be relative to this area to compensate for potential apparent movement due to snow accumulation and melt. The assumed stability of this area is consistent with regular historical monitoring by BC Hydro.

2.4.2 Validation of GB-InSAR Results

To validate the results of the analysis, the discontinuous GB-InSAR data were compared to and validated against surficial deformation measurements with a range of accuracies and temporal frequencies, including in-ground instrumentation, survey points, and other remote sensing datasets. Figure 2-8 shows the GB-InSAR LoS cumulative displacement map for November 15, 2016 to March 4, 2019 relative to a stable area to the north of the slide area. The radar image unfortunately does not cover the entire rock face at the toe of the slope due to the current radar orientation, protective window, and ground conditions including snow cover; these all contribute to a reduction in image coherence, i.e., data quality and reliability. The upper vegetated portion of the slide within the view of the radar was chosen to be included in this analysis to assess the ability of the GB-InSAR to quantify movement in this area; however, this resulted in significant temporal decorrelation and greater than anticipated displacements (circled in red, Figure 2-8) when compared to in-place instrumentation data. This is likely a result of the relatively low coherence in this area compared to the rock cut at the toe of the slope due to the dense vegetation, ground cover, lower incidence angle, and relatively deeper snowpack in flatter areas.

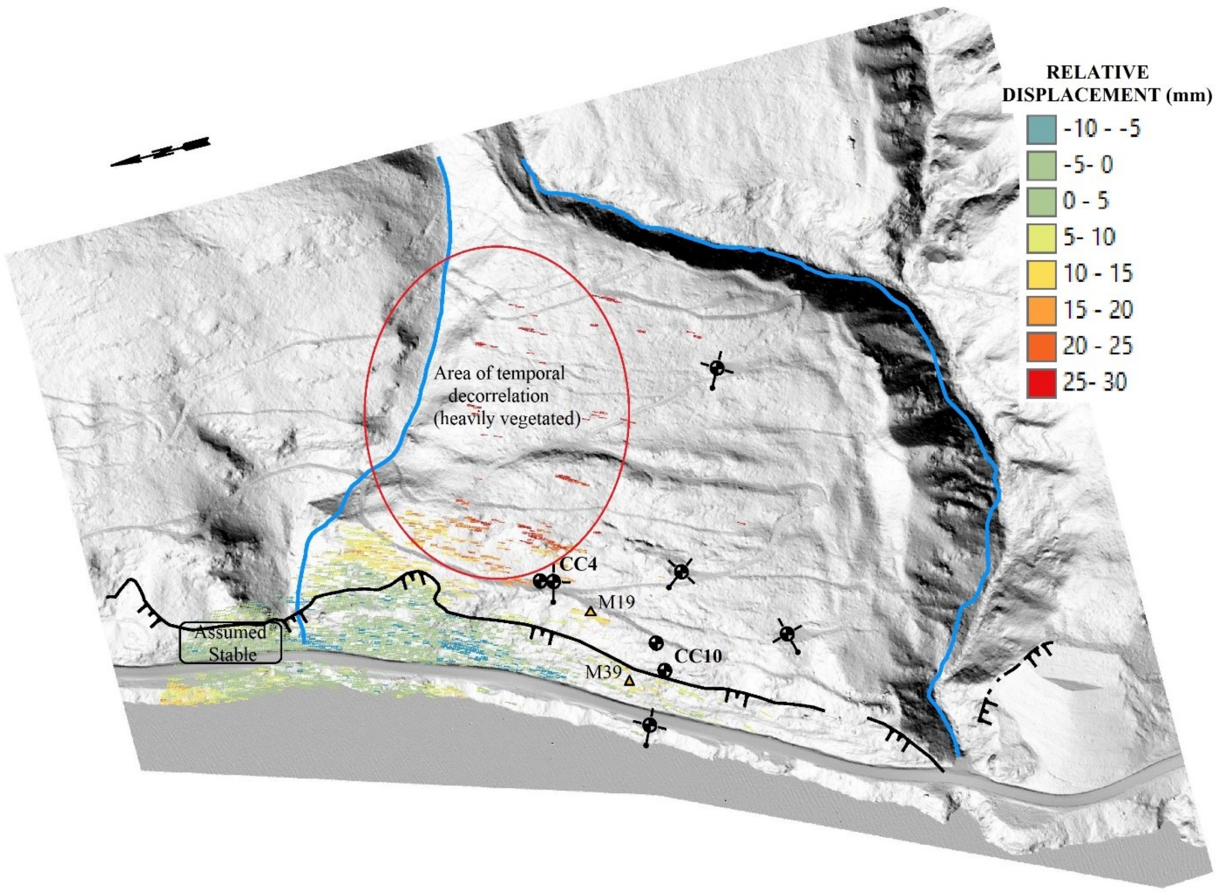

Figure 2-8: GB-InSAR cumulative LoS displacement map between November 15, 2016 and March 4, 2019. Locations of extensometer CC10 and slope inclinometer CC4 are noted.

Figure 2-9 plots GB-InSAR vs. instrumentation data from the area in the immediate vicinity of the corresponding instrumentation. The time of each data point corresponds with the best match SAR image selected for analysis. The displacements measured at location CC10 correspond to the extensometer section representative of displacements at the surface despite not being the shallowest instrument (3.2 m depth), and its displacement rate is equivalent to the average rate of movement of a nearby survey point (M39). Figure 2-8 also shows the location of an inclinometer in drill hole CC4. The data plotted for this inclinometer represent the average cumulative displacement at the surface over the monitoring period. Average values were used as SI readings in August 2018 of several inclinometers showed significant apparent negative (backward) displacements that were not believed to be representative of the true displacement over that time period as it did not agree with other instrumentation. Displacement values from the previous 5 annual SI readings of CC4 however were consistent with the average cumulative values and other instrumentation.

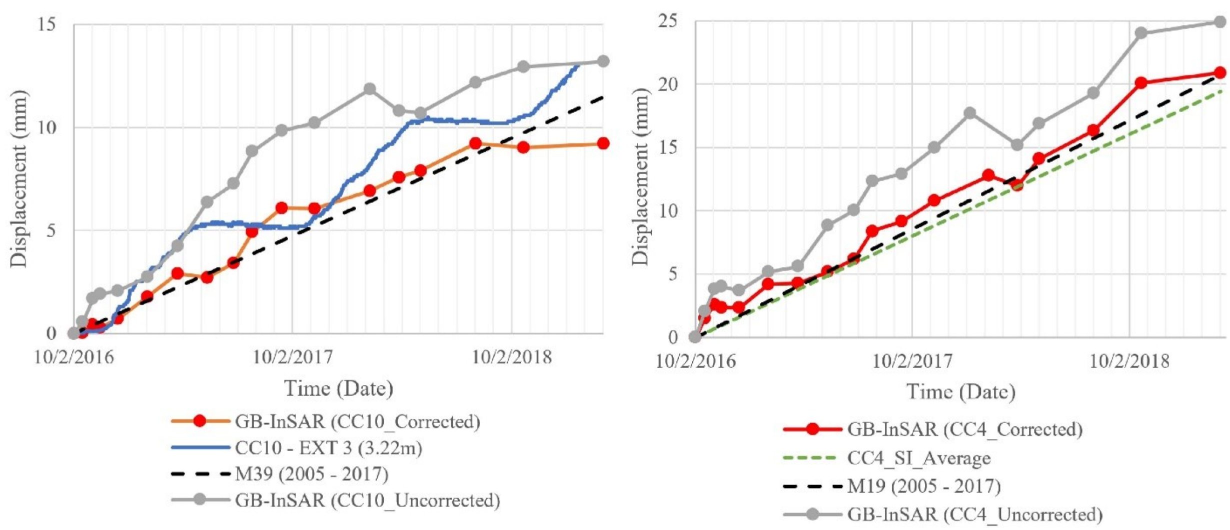

Figure 2-9: Cumulative displacement in LoS direction by discontinuous GB-InSAR in the vicinity of extensometer CC10 (a) and slope inclinometer CC4 (b) and average displacement of nearby survey monuments.

As shown in Figure 2-9, the GB-InSAR results in the vicinity of CC10 started accelerating at approximately the same time as the extensometer measurements for CC10 (between December and January). Further, the magnitude of displacement in this area is consistent with measured displacements at CC10 and CC4 and the average rate of the nearby survey points, M39 and M19 Figure 2-9). That being said, the seasonal displacement pattern obvious in the extensometer data does not appear to be nearly as defined in the GB-InSAR data, potentially due to its relative lower measurement frequency and lower measurement accuracy. Unfortunately, other instruments located above the rock face that have higher frequency data were not able to be used for validation as data was not sufficiently coherent in these areas. As well, in-place-inclinometer data (IPI) with high measurement frequencies could not be used as they are located well below the surface of the slope (at a depth of approximately 33 to 49m).

2.4.3 Statistical Analysis of GB-InSAR Results and Sources of Error

The analysis of the discontinuous GB-InSAR data was completed by taking the mean LoS displacement values from a chosen area in the vicinity of known in-place instrumentation on the

2D displacement map and correcting them relative to the mean values within a known stable area. However, the values reported are average values within those areas and therefore have some inherent variability over numerous pixels within both the stable area and selected area of interest on the displacement map. Therefore, based on the number of pixels within the area, the mean value, and standard deviation of the datasets, a confidence interval (CI) for the GB-InSAR results was determined using:

$$CI = \pm z \times \sigma/\sqrt{n} \text{ , [1]}$$

where z is the z-value (1.96 for 95% CI), σ is the standard deviation, and n is the number of data points. The 95% confidence interval chosen in this assessment can be used to set a probable upper and lower bound of the GB-InSAR results for an area such as in Figure 2-10. As each subsequent displacement map between monitoring campaigns is cumulatively added in this analysis, the range of the upper and lower bounds of the confidence interval increases over time as the error accumulates (Figure 2-10).

Other potential sources of error within the data beyond the spatial variability could also impact these results. For one, the boundaries chosen for the stable area and area of interest in the vicinity of instrumentation are relatively arbitrary. Choosing a larger or smaller collection of pixels in these areas could impact the results of the analysis. The coherence (or quality) and strength of the backscattered signal from a particular area depending on the surface characteristics (e.g., vegetation, geometry) will also impact the accuracy of these results; further filtering of lower quality data may improve this but would reduce the spatial coverage. Atmospheric effects such as cloud, rain, and other weather can also impact the results, but are compensated for during acquisition of the data by internal processing algorithms. Details of how the processing of atmospheric effects on the resulting data and related errors are outside the scope of this paper and are commonly proprietary to the software developer.

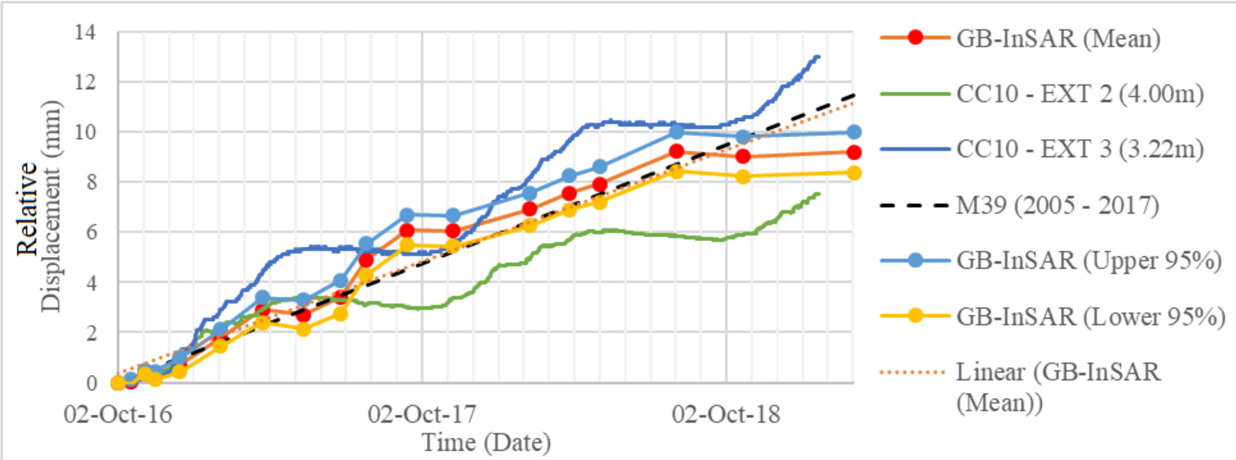

Figure 2-10: Statistical analysis of GB-InSAR results.

2.4.4 Impact of Snow Accumulation and Melt

The presence or lack of presence of snow within the monitored area may also impact the resulting data and associated level of error and is a particular concern at the site considered in this work. To assess the impact of snow accumulation and melt within the monitored area on the GB-InSAR results, the apparent displacements of an area between monitoring campaigns both with and without snow were compared to the anticipated displacement based on historical instrumentation data trends. To confirm the presence or lack of snow on the rock face, weather data including temperature and precipitation as well as site photos were referenced.

Since the start of the GB-InSAR monitoring of the site, three winter freeze-thaw cycles have occurred (winters of 2016/17, 2017/18, and 2018/19), see Table 2-4. If snow significantly affected the results, the apparent ground movement would be much greater than expected during the fall as the snow accumulates and much less (potentially in the negative direction, away from the sensor) during the spring as the snow melts. For ease of comparison, data from the assumed stable area (Figure 2-8) were used to determine the impact of snow on the GB-InSAR results; without the contribution of some source of error (such as snow) the average displacement in this area is expected to be zero. The resulting maps of the stable area had an average apparent displacement of −0.2 mm between all monitoring campaigns, which is within the expected level of error given the target's distance and geometric characteristics.

Table 2-4: Snow accumulation and melt impact of GB-InSAR results

Winter Period	Monitoring Campaigns	Dates	Apparent Movement (mm)	Notes
Fall 2016 Accumulation	MC4 to MC6	Nov. 23, 2016 to Dec. 11, 2016	0.25	Freezing temperatures starting Nov. 26. Snow present in site photos from Dec. 11.
Spring 2017 Melt	MC8 to MC9	Mar. 25, 2017 to May 12, 2017	**-2.34**	Site photos show snow nearly completely melted as of May 12.
Fall 2017 Accumulation	MC14 to MC15	Jan. 15, 2018 to Mar. 26, 2018	**1.70**	Limited snowfall in early winter, weather data and site photos show no significant snowfall until late Jan.
Spring 2018 Melt	MC15 to MC16	Mar. 26, 2018 to May 2, 2018	0.44	Site photos from May 2 show face completely free of snow.
Fall 2018 Accumulation	MC18 to MC22	Oct. 24, 2018 to Nov. 19, 2018	-0.44	Some snow on face starting Nov. 10 and remaining until May.
Spring 2019 Melt	MC22 to MC23	Apr. 26, 2019 to May 8, 2019	Not available	InSAR data from Spring 2019 (MC23) have yet to be processed.

If the campaigns with snow accumulation and melt are isolated from the entire dataset (Figure 2-11), two outlying data points appear to have significantly greater displacements than expected: spring 2017 melt (March 25 to May 12, 2017) between MC8 and 9 and fall 2017 snowfall (January 15 to March 26, 2018) between MC14 and 15 (Figure 2-11). Comparing these two periods to accumulated precipitation data for the site, there is an apparent large increase and decrease in apparent movement of the stable rock face (Figure 2-12). However, to determine whether these two data points represent a true statistical variance from the rest of the dataset, the inter-quartile range (IQR) was calculated, i.e., the range between quartiles 1 and 3. The IQR was then multiplied by 1.5, which is a common tool to determine if a certain data point is an outlier or not:

$$Q1\text{-}Q3=IQR \times 1.5, \qquad [2]$$

This resulted in apparent displacements greater than ±1.2 mm in the stable area to be classified as outliers. The two values in question thus represent a significant deviation from the mean and indicate that snow accumulation and melt may have had a significant effect on the results over those time periods. However, apparent movement of the stable area over other periods of snow accumulation and melt (fall 2016, spring 2018, and fall 2018) are within these bounds and are therefore not considered statistical outliers and does not appear to have significantly affected the analysis of the discontinuous GB-InSAR data. This may be due to several factors, including sufficiently dry or shallow snowpack conditions at the time of the scan, allowing the radar to penetrate and therefore return signals from the actual ground surface rather than the snow surface or within the snowpack. For example, the winter period of 2016/17 had a significantly higher than average snowfall (approximately 1150 mm vs. 600 to 800 mm on average) however, only a small percentage (approximately 15 mm or 13%) of the annual snow fall for that year had occurred before the time of the second scan in December 2016, see Figure 2-12. This resulted in a shallower snowpack during scanning which is reflected in site photos at that time. Similar can be said about the winter period of 2018/19, which had a significantly lower than average annual snowfall, approximately 17% of the average winter precipitation. However, it is unclear why there would be no impact from the melt of spring 2018 as that year represented only a slightly below average snowpack and weather data and site photos confirm the site had a significant snowpack at the time of the first scan and was largely bare during the second, see Table 2-4.

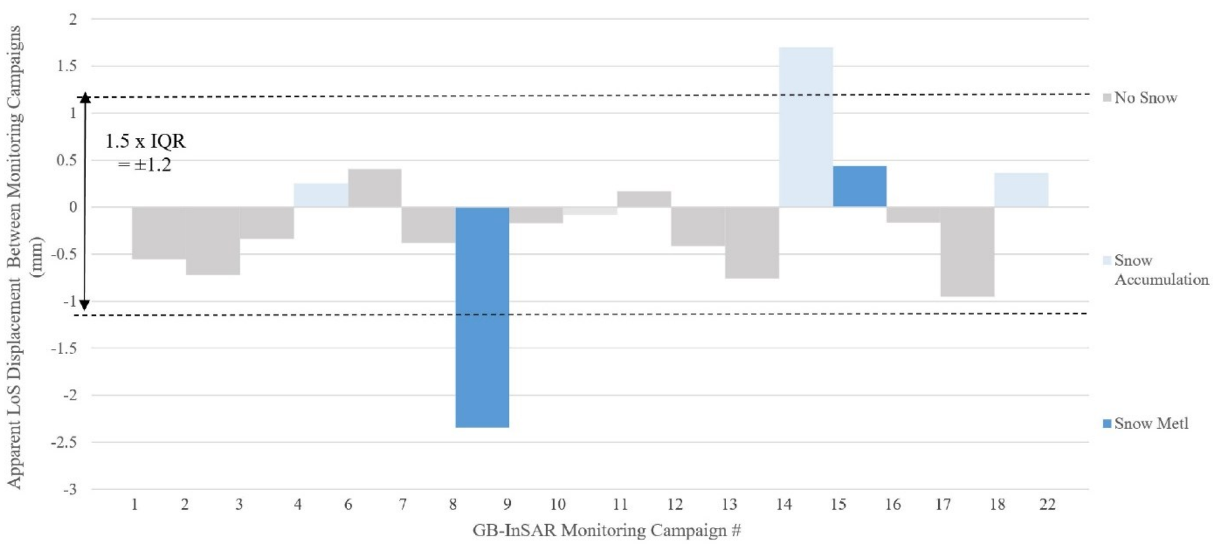

Figure 2-11: Impact of snow accumulation and melt on apparent LoS displacement

Despite this, the analysis shows that the presence of snow on the rockface can have a significant effect on the results of discontinuous GB-InSAR monitoring, such as during winter months; this aligns with results during continuous monitoring reported by Dehls et al. (2010) and Carlà et al. (2019). However, by subtracting apparent movements from an assumed stable area within the study site can compensate for this during post-processing, such as was done in ArcMap to verify the results of this analysis. Doing so appears to significantly increase the correlation of the GB-InSAR data with the in-place instrumentation data as shown in Figure 2-9. That being said, the snowpack within a given area can have a highly variable thickness and material properties depending on site conditions. Therefore, the presence of snow can contribute to an increased level of error in comparison to periods of no snow that is difficult to quantify and may impact the equipment's ability to accurately monitor the area continuously over the winter months. Therefore, greater scrutiny of these results and validation of this data to other instruments should be done over these time periods.

Figure 2-12: Accumulated precipitation over winter months vs. apparent movement of stable area

2.5 Conclusions

This paper provides an overview of GB-InSAR in its use of monitoring slopes in remote mountainous environments with vegetation and seasonal snow-cover, including its advantages and limitations. These technical limitations and logistical challenges have been assessed at the Checkerboard Creek Rock Slope in Revelstoke, BC, Canada.

GB-InSAR monitoring offers many advantages including its ability to capture a large area of high-frequency, highly accurate, continuous displacement data, in all weather conditions. Short-term (approximately 1-2 week) monitoring campaigns between November 2016 and March 2019 were used to calculate relative slope displacements with D-InSAR processing methodologies. Challenges associated with coherence loss due to vegetation remain, but post-processing of the resulting data by comparing results to an assumed stable area appears to compensate for apparent movements due to snow accumulation and melt and is consistent with instruments in the vicinity of the rockface at the lower portion of the site. This includes agreement on maximum surficial displacement rates of approximately 10 mm/y for extensometers, slope inclinometers, and GB-InSAR data in the same vicinity.

In addition, recent efforts have successfully addressed power availability and telecom issues in a cost-effective and reliable manner and allowed the acquisition of continuous data for potential future near real-time monitoring and early warning purposes. Overall, findings of this research verify the feasibility of implementing GB-InSAR to monitor slopes at sites with similar conditions given considerations including limitations and logistics associated with snow cover are addressed.

3 PAPER 2: Updated understanding of the deformation characteristics of the Checkerboard Creek rock slope through GB-InSAR monitoring

This chapter was revised and submitted for publication under the title *Updated understanding of the deformation characteristics of the Checkerboard Creek rock slope through GB-InSAR monitoring* (Woods et al. Submitted) in the International Journal on Engineering Geology on May 27th, 2020.

3.1 Introduction

Ground-based, interferometric, synthetic aperture radar (GB-InSAR) has been successfully implemented for the monitoring and assessment of both natural and man-made slopes (Atenzi et al. 2014, Barla et al. 2011, Dick et al. 2015, Tarchi et al. 2005). It can produce high resolution (spatial and temporal) continuous data that can be used to provide new insights and a greater understanding of displacement trends/patterns, triggering mechanisms, and failure kinematics of landslides when compared to more conventional, point-wise, and low-frequency monitoring techniques such as slope inclinometers and other in-place instrumentation. However, this technology, and other remote sensing techniques like it, have limitations in their efficacy particularly in their application in monitoring natural, vegetated, and snow-covered slopes.

Recently, this technology has been applied to a slow-moving (average rate of displacement of ~10 mm/y) 2 to 3 million m^3 bedrock landslide known as The Checkerboard Creek Rock Slope located near Revelstoke, BC, on the Revelstoke Reservoir, just upstream of BC Hydro's Revelstoke Dam.

This paper presents the results and interpretation of recent remote monitoring at this site and potential new insights it may provide on its activity, kinematics, and failure mechanism(s) in comparison to current understanding based on previously completed numerical modelling, as well as observations and hypotheses developed from in-place instrumentation data. However, this site poses many challenges and limitations regarding reliable implementation of GB-InSAR. Details on the solutions for the successful operation of the equipment at this site and validation of the results through a comparison with existing geotechnical instrumentation is provided in a separate paper (Woods et al. 2020).

3.2 The Checkerboard Creek Rock Slope

The Checkerboard Creek Rock Slope is located approximately 1.5 km north of the Revelstoke Dam on the Columbia River along Highway (Hwy) 23, upslope of the eastern shore of the Revelstoke Reservoir (Figure 2-3). The reservoir is for hydroelectric power generation purposes with a surface area of approximately 115km^2, oriented roughly north-to south with the Revelstoke Dam to the south end and Mica Dam at its northern extent, both of which are owned and operated by BC Hydro (Salmon 1988). Revelstoke Dam itself is located about 5 km upstream of the town of Revelstoke, British Columbia (BC) and is a composite dam comprised of an approximately 1160m long earthfill embankment section on the north side and a 185m long concrete gravity dam and spillway structure to the south (Taylor and Lou 1983; Salmon 1988).

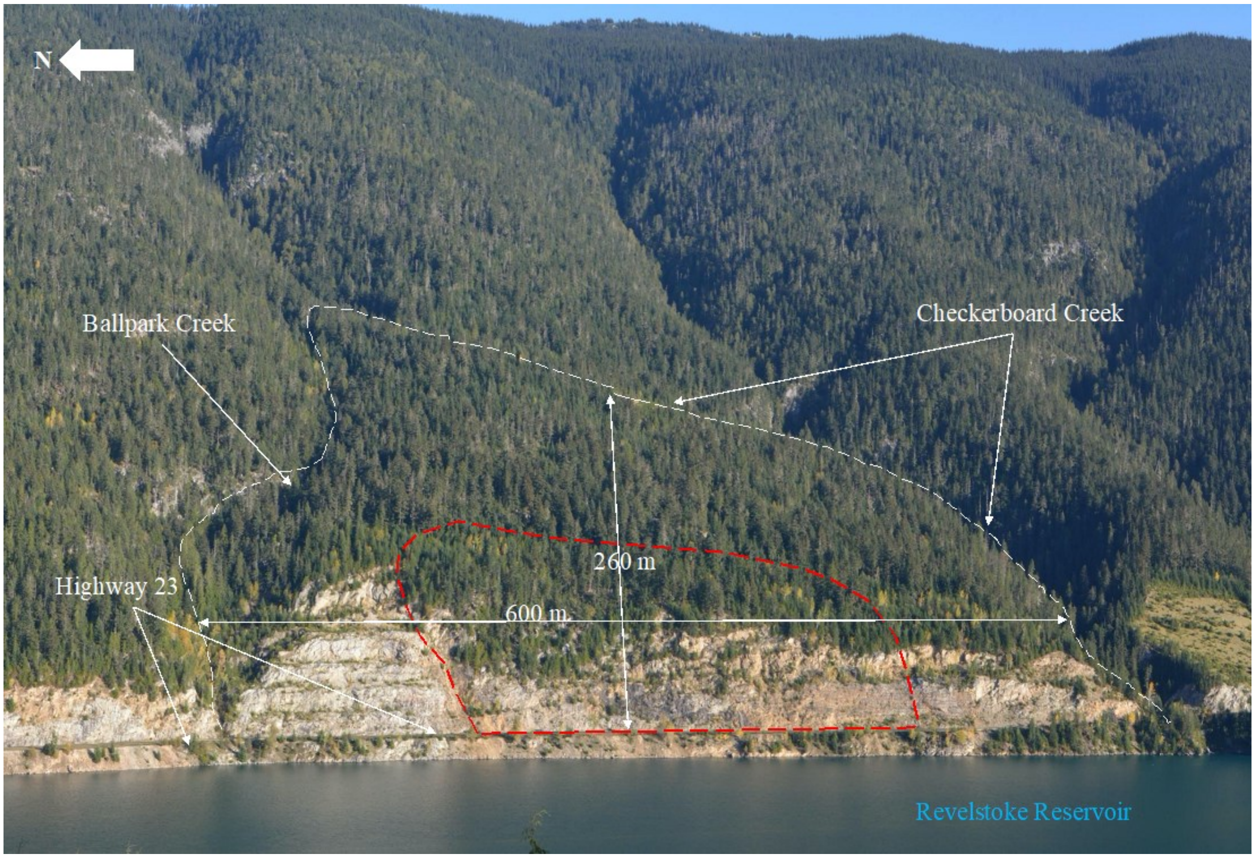

Figure 3-1: Checkerboard Creek Rock Slope Elevation viewed from west side of Revelstoke Reservoir

In its current condition, the elevation at the toe of the Checkerboard Creek Rock Slope at Hwy 23 is about 260 m, rising eastward up to 590 m at its crest. It is bounded on its eastern uphill side by the upper reaches of Checkerboard Creek (Figure 3-1) which runs parallel to the slide crest. It is bounded to the south by the lower reaches of Checkerboard Creek after it turns and flows directly downslope. To the north it is bounded by Ballpark Creek, which flows intermittently, and to the west by the Revelstoke Reservoir. The slope itself is approximately 600 m wide with an overall slope angle of 30°; however, it is steeper at the toe (45°) near the rock cut excavated for Hwy 23 and relatively flatter in the upper area (25°) (Watson et al. 2004).

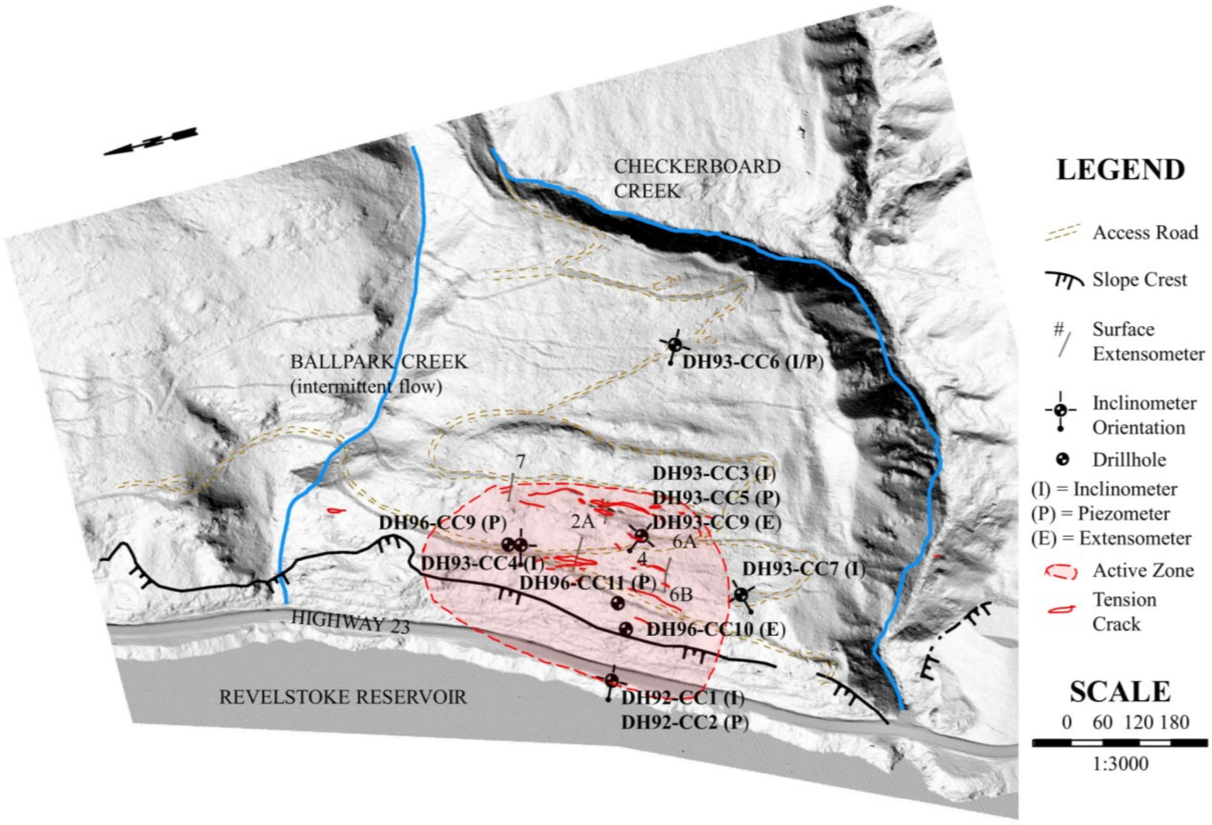

Figure 3-2: Drillhole (CC1 to CC11) and surface cable extensometer locations (LiDAR hillshade image generated from 2014 BC Hydro survey) (from Woods et al. 2020)

An area of active movement of the slide has been interpreted from the site geology, slope topography, and deformation patterns (Macciotta et al. 2016). This area is located towards the central lower portion of the rock slope and is approximately 200 m wide along the direction of Hwy 23 and 150 m deep from the highway to the uppermost tension cracks that define the upper boundary of the deformation area (Figure 3-2). However, the lateral and toe boundaries of this area are less well defined. Therefore, one goal of the analysis of the GB-InSAR monitoring was to better define these boundaries. The active zone of deformation has an average slope angle of 45°, and deformations have been detected down to 50-60 m deep within a zone of higher weathering and lower quality rock masses. The total volume of this active zone is estimated somewhere between 2 and 3 million m^3.

3.2.1 Site History

Construction of the Revelstoke Dam occurred between 1977 and 1984 and the subsequent impoundment of the reservoir necessitated the relocation of Hwy 23. Whereas other larger areas of instability farther upriver of the dam had been identified prior to construction, such as the Downie Slide, which was first observed in the 1950s during reconnaissance mapping for proposed dam sites on the Columbia River (Blown 1966), no obvious stability concerns were recognized in the area of Checkerboard Creek prior to excavation for the highway relocation works. Prior to relocation works, investigation of the slope was limited to surface mapping which noted the hard, strong igneous rock outcrops which largely dominated the slope in the area of the proposed rock cut (Moore 1999). However, at the time, no note was made of the post-glacial tension cracks in the forest uphill of the excavation. Therefore, the initial rock cut design for the highway consisted of a series of 15.2 m high, near vertical faces sloped at 1 :4 (H;V), with 3.0 m wide benches (Stewart and Moore 2002).

As excavation began in 1978, it was revealed that rock beneath the surface was fractured, weathered, and loose which required the slope to be stabilized with a vast amount of rock support and flattening slopes as much as practically possible (Moore 1999). Later in 1984, detailed slope investigations were initiated following the discovery of apparently fresh tension cracks about 70m uphill of the excavation (Stewart and Moore 2002).

3.2.2 Site Geology

The geology of the Checkerboard Creek Rock Slope primarily consists of massive to slightly foliated granodiorite overlying the easterly dipping gneiss and schist of Columbia River Fault; a broad, regional, brittle deformation zone of altered and mechanically deformed rock (Lane 1984) that becomes progressively more pronounced with depth. Primary fault zones dip east into the slope and, based on prior analyses, appear to place an indirect role in the kinematics of the slope displacement (Stewart and Moore 2002).

Structure in the slope is primarily dominated by two well-defined joint sets and the fault zones described above. These orthogonal joint sets dip steeply (greater than 80 deg), with the primary set generally parallel to the slope and the secondary set perpendicular (Stewart and Moore 2002), however, there is no evidence of a downslope dipping base of sliding (Watson et al. 2006).

Surface features on the slope including open tension cracks (discrete, planar to sinuous bedrock cracks within outcrops, or collapse features with thin surficial deposit cover) and partially infilled bedrock linears are exposed at the central area of the slope and trend sub-parallel to the slope between approximate elevations of 650 and 740 m (Macciotta et al. 2016). Bedrock linears are wide (up to 15m) gullies, benches, and uphill facing scarps and are consistent with features of similar morphology in the Columbia River Valley, BC, and other mountainous regions. Evidence at the site suggests the origin of these features appears to be related to both erosional and gravitational processes as subsurface exploration indicates that the bedrock has been glacially scoured along zones of weakness (faults and fractures) and infilled by glacial and colluvial deposits (Stewart and Moore 2002).

Rock mass quality is highly variable and ranges from very strong, fresh, undisturbed, and blocky to highly weathered, altered, weak, and disturbed (Macciotta et al. 2018). This poor-quality rock is typically restricted to depths within 60m of the slope surface, where active displacements have been observed. The rock quality below this depth is generally fair to good, with localized zones of poor rock along shear and fault zones (Stewart and Moore 2002).

3.2.3 Groundwater Conditions

Groundwater levels in the slope have been inferred from observations during drilling, site inspections, in-situ testing, and monitoring of multiple piezometers. These have revealed a complex "compartmentalized" groundwater regime, related to low-permeability shear zones, and with saturated conditions at a depth of 50 to 80 m below the slope surface (below the base of the active slope deformation). Seasonal variations in piezometric level within the slope typically can be up to 20m and are greatest towards to the top of the continuously saturated rock mass (Stewart and Moore 2002). Generally, the piezometric data suggest that a downward pressure gradient exists, with the main source of recharge occurring from infiltration (Watson et al. 2006) displaying a direct response to precipitation and, to a lesser degree, seasonal snowmelt (Stewart and Moore 2002) and not to regional groundwater flow.

Increases in piezometric levels in the upper zone of the slide typically have a 12 to 18-hour lag time following precipitation, with a progressively greater lag time with increasing depth. These levels display a sharp increase that is primarily associated with autumn-early winter precipitation and spring snowmelt, followed by a decreasing trend during spring to early autumn (Stewart and Moore 2002). These transient groundwater flows and pressures in the upper weathered zone of the rock mass are considered as a possible trigger for observed seasonal slope displacement cycles.

3.2.4 Site Climatic Conditions

Annual precipitation at site typically ranges between 1500 to 2000 mm, approximately 40% of which occurs between October and January, mostly as snow. Air temperatures typically range between −25 and 35 °C, with freezing temperatures prevailing from late November through March. Because the slope is heavily vegetated with large trees, snow depths can be highly variable but typically range from 1 to 2 m in mid-winter (Watson et al. 2004). The fall and winter days at the site feature short periods of sunlight, fog, frequent overcast weather, and snowfall events between December and March.

3.2.5 Slope Displacement Trends

Slope monitoring has revealed generally very slow annual displacements that have remained relatively consistent with average downslope rates of 5-15mm/y (Stewart and Moore 2002). The displacement rate is as little as 0.5 mm/y at the boundaries of the active area and up to 15 mm/y within the most active area. These rates are greatest at the surface and decrease progressively with depth.

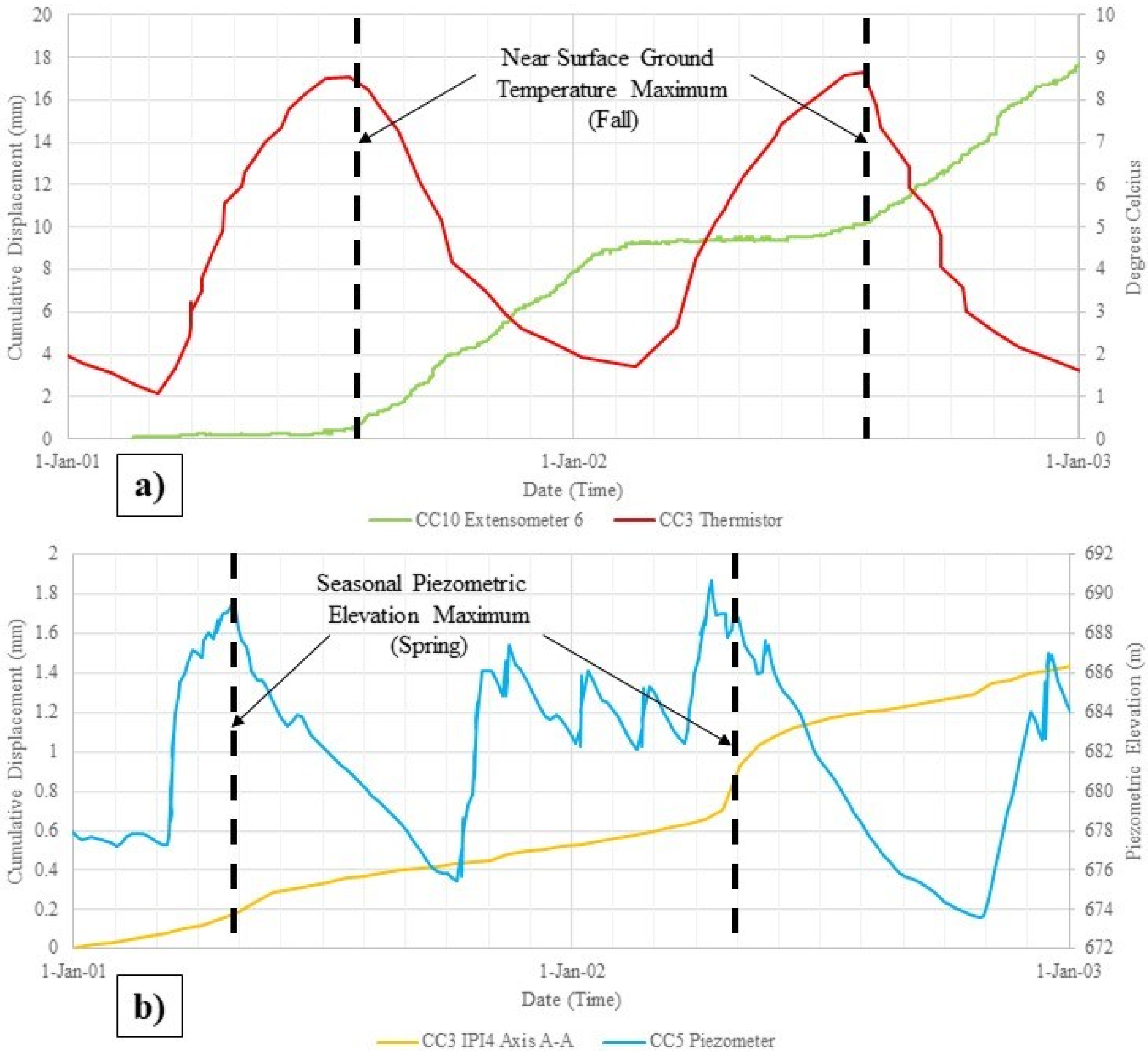

Figure 3-3: Seasonal displacement pattern vs. sub-surface temperature fluctuation a) and piezometric level b)

Instruments with high measurement frequencies near the exposed rock face at the toe of the slope have indicated a persistent annual seasonal displacement pattern with accelerated movement in the early fall to late winter and reduced displacements in the spring and summer (Stewart and Moore 2002; Watson et al. 2004, 2006), see Figure 3-3. However, instrument trends further back in the landslide and at depth have a steadier displacement. Interpretation of this displacement pattern shows an accelerated phase during spring snowmelt, when piezometric pressures are at seasonal maximums, as discussed previously, however, investigations regarding the possible cause(s) of the acceleration are ongoing.

The deformations are generally widely distributed within the deforming mass but zones where these are more concentrated or absent also exist. These patterns indicate deformations may be due to dilation of the rock mass due to seasonal temperature changes with discrete block sliding and rotation occurring throughout the mass (Stewart and Moore 2002; Watson et al. 2004, 2006) rather than sliding as a single cohesive block along a failure plane or simple toppling (Macciotta et al. 2016). Geomorphic evidence such as tension cracks indicates a long history of surface displacement of up to 10 m or more (Watson et al. 2006) that have developed over a time scale of at least hundreds of years (Stewart and Moore 2002).

3.2.6 In-place Instrumentation

An extensive amount of in-place slope instrumentation exists at this site, mostly installed between 1984 and 2000 (Watson et al. 2006). The locations of most of these instruments are shown in Figure 3-2 and a detailed summary is provided in Table 2-2. Monitoring instrumentation includes surface electronic distance measurement (EDM) survey monuments which are read annually, manually-read slope inclinometers (annually) and in-place slope inclinometers (IPIs, every 6 h), nested standpipe piezometers, multipoint borehole extensometers (every 4 h), surface cable and extensometers (annually), strain meters, borehole and surface thermistors, and a weather station that records daily temperature and precipitation values (Macciotta et al. 2016).

Many of these instruments have been incorporated into an automatic data acquisition system (ADAS) that is continuously monitored from Revelstoke Dam. This instrumentation network was established to develop a detailed understanding of the slope's displacement behavior and the hazard associated with a potential slope failure, and to provide early warning for changes from a slow seasonal displacement behavior into a more rapid failure (Stewart and Moore 2002). However, the current displacement rate only exceeds the measurement sensitivity of the inclinometers after about 6 months as the annual displacement rates are very small and distributed over wide areas within the deforming rock mass (Watson et al. 2006).

The most sensitive and high frequency displacement measurements from in-place instrumentation at this site are currently restricted to the multi-point extensometers (drill holes

CC8 and CC10), IPIs (CC3 and CC4), and a single laser distance measuring device located on the slide surface (6B). However, all these instruments only provide data for a single point at specific depths for each respective location. Furthermore, the IPIs are installed at a greater depth (minimum 32.5m below ground surface, drillhole CC4 – IPI 1) toward the base of the active zone and therefore have a much slower rate of displacement that is unrepresentative of the total displacements recorded at surface. Due to the relatively low frequency of the other instrumentation, observation of the seasonal displacement pattern discussed in Section 2.5 has been largely restricted to a selection of these instruments, namely: CC3 IPI 2. CC4 IPI 4, CC8 Extensometers 2-6, CC10 Extensometers 1-6, and the laser distance monitor.

These restrictions demonstrate the need for a highly accurate monitoring system that can cover a large area. Therefore, several types of remote sensing have been employed at this site by BC Hydro, including a global navigation satellite system (GNSS) network with four sensors located at different locations around the site and airborne and terrestrial laser scanning (ALS/TLS). GB-InSAR monitoring has been operational at site since October 2016 and is described in further detail in Section 3. TLS and UAV photogrammetry surveys were also completed on several occasions from 2015 to 2019, however are not included in this analysis outside of visualizations of the site.

3.3 Slope Stability Modelling

Since the slope stability concerns and this landslide have first been identified at this site as discussed in Section 2.1, several iterations of numerical modelling have been completed for a variety of analytical purposes such as to increase understanding of the landslide failure mechanism, kinematics, runout distance, probability of rapid failure, seismic stability, etc. This section discusses a few of the methodologies used to model this slope, how they compare and contrast, and their results so they may be compared to the results of the GB-InSAR analysis and interpretations of those results.

3.3.1 Preliminary Numerical Modelling (FLAC)

These studies were completed on behalf of BC Hydro using FLAC (Fast Lagrangian Analysis of Continua) numerical modelling software to develop a more comprehensive understanding of slope deformation behavior and forecast behavior during anticipated future loading conditions (Moore et al. 2001). However, this demonstrated a continuum approach that was unable to fully capture the pattern of displacements and pore pressure measurements discussed in Section 2 (Watson et al. 2006).

In this case, the rock slope was modelled as a continuous material using a two-dimensional plane strain approach, based on Mohr-Coulomb, elastic plastic formulation that is dilational upon yield. The rock mass was generalized into three types Good quality, Fair quality, and Poor to very poor conditions. Each type had assigned ranges of unconfined uniaxial strength (UCS), Geological Strength Index (GSI), and depths with the poorest rock mass quality localized in the upper 60m of the slope and area of active slope displacement. Groundwater conditions were modelled with a phreatic surface to simulate continuous saturated conditions and with applied pore pressure in the displacing zone to simulate seasonal transient conditions (Moore et al. 2001).

This modelling resulted in marginal stability under 'dry' summer groundwater conditions, and unstable under 'wet' fall-winter groundwater conditions consistent with the observed magnitude and pattern of slope displacements and was very sensitive to changes in groundwater conditions in the upper rock mass. Slope displacements were characterized by an overall rotational mechanism, consistent with toppling, involving shear and tensile yield along ubiquitous joints and long-term behavior of the slope model indicated that displacement rates consistent with current monitored magnitudes are likely to continue for some time (Moore et al. 2001).

3.3.2 Discrete Element Analysis (UDEC)

The Discrete Element Analysis of this site was completed by Itasca Ltd. using UDEC (Universal Distinct Element Code) modelling software, the objective of which was to investigate the post-failure behavior of the slope in order to estimate possible rock volumes that could enter the reservoir and generate a wave that could pose a hazard to the Revelstoke Dam (Lorig et al. 2009).

This methodology was selected for its capability to include joints and shear zones explicitly with groundwater flow restricted to these joints, as well and the ability to model thermal and dynamic loads (Watson et al. 2006). Two phases of numerical analysis were completed at this time with the first phase investigating the annual displacement pattern and stability of the slope during a 1-in-10,000 year seismic event. The second phase investigated the runout potential of the slope which is not discussed in this paper.

The UDEC stability analysis included all observed geological units, shear zones, faults, joints and rock mass weathering considered significant to overall slope behavior (Watson et al. 2006) along with additional sub-vertical joints.

Significant effort was spent exploring the potential driving mechanism for the observed displacement pattern. With model calibration along with measured groundwater distribution and annual temperature fluctuations, the UDEC model eventually produced annual cycles similar to those measured in the extensometers and IPIs (Watson et al. 2006). Resulting displacements were very sensitive to input parameters, namely the interpreted extent of the perched water table and thermal coefficient of expansion and elastic modulus of the rock mass, as well as the discontinuity strength (Lorig et al. 2009).

The UDEC analysis showed that thermal contraction during cooling of the near surface bedrock introduced deviatoric stresses into the slope which could cause slip along discontinuities. It was hypothesized that this slip may occur in response to a reduction in effective normal stress allowing wedges formed by steeply dipping discontinuities to cause outward, downslope movement (Watson et al. 2006). In contrast, during warming and expansion, normal stresses increase which limits further slip, see Figure 3-4. The resulting spatial distribution of displacements from this modelling caused by changes in ground temperatures reasonably matched those measured in the slope by in-place monitoring. This modelling also confirmed that the most vulnerable part of the slope was the over steepened rock cut located immediately about the highway.

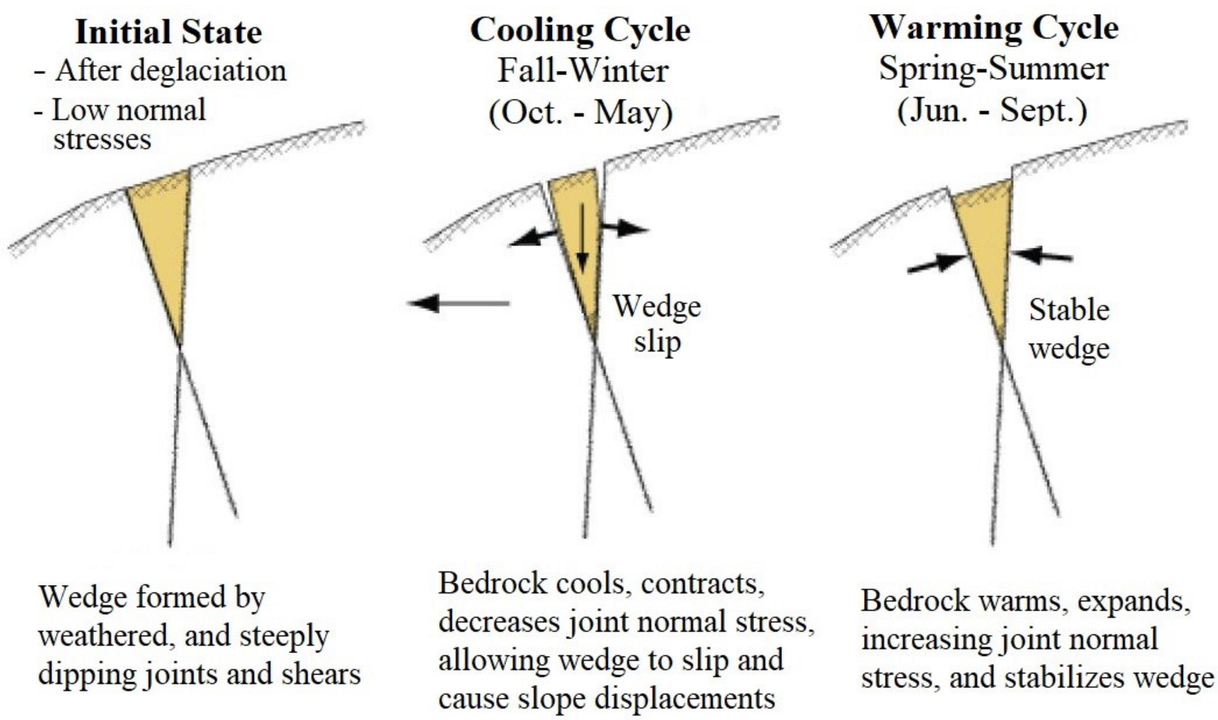

Figure 3-4: Hypothesized temperature-driven slope deformation mechanism (from Martin et al. 2011)

3.3.3 Damage Model (UDEC-DM)

Subsequent to the initial UDEC modelling described previously, this modelling was carried out using a discontinuum approach that could accommodate discrete fractures and growth of new fractures that are required as part of the proposed yield mechanism (Martin et al. 2011). However, this analysis differed by utilizing a discrete element approach without artificial conjugate joints i.e. failure is restricted to natural joint sets and failure of intact blocks. Input parameters for this modelling were the same as previous. In addition, the effect of weathering on the rock mass in this modelling was simulated by gradually reducing its tensile strength in increments until unstable deformation developed. Ultimately, this modelling approach resulted in a similar failure mechanism and spatial distribution of displacements to the previous UDEC modelling, however with a significantly less volume of collapsed rock. A constant velocity boundary was also used to model the effect of long-term movements on slope stability, resulting in a total horizontal displacement of 1.8m or 180 year period required to induce collapse.

3.4 GB-InSAR Monitoring

Like typical radar systems, GB-InSAR is based on the concept of transmitting electromagnetic waves from a scanner to a target (in this case the ground surface) and receiving reflected waves to determine the distance and direction from the scanner to the target by evaluating the time of flight of backscattered waves (Atzeni et al. 2014). This type of radar systems takes the received radar signals and arrange them in a two-dimensional (2D) image map of one-dimensional line-of-sight (LoS) distances (Lombardi et al. 2017). Two radar images of the same scene taken at different times can then be used to generate interferograms, i.e., wave phase difference images (Wasowski and Bovegna 2014). These interferometric images can then be related to a change in position (i.e. displacement) and then presented in three dimensions (3D) by overlaying the displacement map over a digital elevation model (DEM) (Atzeni et al. 2014), such as those derived from ALS, TLS, and photogrammetric methods. Atmospheric correction methodologies are then applied to the raw data to compensate for the effect of weather conditions such as rain, snow and fog. Further details about the technology and data processing can be found in Atzeni et al. (2014), Wasowski and Bovegna (2014), Colesanti and Wasowski (2006), and Ferretti et al. (2007).

GB-InSAR has some inherent advantages when compared to traditional slope monitoring (Crosta et al. 2013) and can be complementary to other techniques (Barla and Antolini 2015; Carlà et al. 2019). These advantages include the ability to provide dense, continuous data, 24 hours a day, in all weather conditions (Lombardi et al. 2017). As well, GB-InSAR data acquisition and processing can be automated and set up as an operational monitoring tool to effectively monitor slopes (e.g., Lombardi et al. 2017).

GB-InSAR data is typically acquired using one of two acquisition modes: continuous (C-InSAR) and discontinuous (D-InSAR) (Monserrat et al. 2014). In C-InSAR, the instrument is left installed onsite to continuously acquire data, typically every 3 to 15 min (Monserrat et al. 2014), allowing for "near real-time" monitoring (Tarchi et al. 2005) of a site. This methodology is appropriate to measure relatively fast deformation phenomena (mm/d to m/d) (Casagli et al. 2003; Tarchi et al. 2003, 2005). For slower phenomena (mm/y) such as the Checkerboard Creek Rock Slope, GB-

InSAR equipment must be either installed onsite and operational over a longer timeframe on the scale of months; or, as an alternative, discontinuous methodologies have to be applied.

Table 3-1: GB-InSAR Monitoring Campaign Details

Monitoring Campaign (MC) #	Start Date	End Date	# of Days	# of Scans	Notes
1	9/29/2016	10/8/2016	9	112	Original Orientation. No window.
2	10/17/2016	10/20/2016	3	39	
3	11/1/2016	11/7/2016	6	69	
4	11/14/2016	11/16/2016	2	220	
5	11/16/2016	11/23/2016	7	71	Radar reoriented. Plexiglass window installed
6	12/11/2016	12/18/2016	7	66	
7	1/31/2017	2/7/2017	7	841	
8	3/23/2017	3/25/2017	2	206	
9	5/12/2017	5/25/2017	13	1564	
10	6/24/2017	7/4/2017	10	1181	
11	7/24/2017	8/7/2017	14	1674	
12	9/9/2017	9/20/2017	11	1305	
13	11/4/2017	11/9/2017	5	557	
14	1/12/2018	1/15/2018	3	337	
15	3/26/2018	3/30/2018	4	525	
16	5/2/2018	5/5/2018	3	301	
17	8/3/2018	8/3/2018	0	16	
18	10/10/2018	10/24/2018	14	1694	New solar panel system installed.
19	11/10/2018	11/12/2018	2	5	Batteries not recharging due to improper wiring
20	11/16/2018	11/16/2018	0	1	
21	12/9/2018	12/9/2018	0	2	Radar no operating. Sent to IDS for repair. Temporarily replace with second GB-InSAR unit.
22	2-Mar-19	26-Apr-19	55	7441	Continuous Monitoring. Data overrun.
23	8-May-19	23-May-19	15	1464	Repairs completed, reinstall original radar. Install hard drive to prevent further data overrun.
24	22-Aug-19	31-Aug-19	9	256	
25	16-Sep-19	?	?	?	Rohacell foam window & new antennas installed

Due to solar power generation restrictions from a lack of sufficient sunlight during winter months, the initial installation of the GB-InSAR at Checkerboard Creek was restricted to data most suitable for D-InSAR from October 2016 to March 2019 as monitoring campaigns were relatively short (1-2 weeks) and with large timespans between campaigns (typically 1-2 months). However, due to recent efforts to improve the power system and other aspects of the installation at Checkerboard Creek, the system was able to provide a longer period of continuous monitoring from approximately March to June 2019, see Table 3-1.

Which data processing methodology is applied for interpretation and analysis purposes is dependent upon which acquisition mode the data was collected. These different processing methodologies are discussed in further detail in Section 4 of this paper.

3.4.1 Installation Details

An IBIS-L GB-InSAR system, owned by the UofA and manufactured by IDS Georadar was installed in October 2016 on top of a rock bluff located on the western slopes of the Revelstoke Reservoir and pointed across the reservoir toward the Checkerboard Creek Rock Slope (Figure 3-1). Access to the site was via a gravel service road, however, was restricted to travel on foot during the winter due to the deep snowpack typically found onsite. The system was installed in a small timber-frame shelter upslope of the access road in order to provide protection from weather and wildlife. While smaller, lighter equipment could be carried up the slope to the shelter, heavier equipment necessitated the use of mobile crane equipment to assist in the shelter installation.

Following installation, the radar was directed through an opening in the east side of the shelter and oriented toward the center and most active area of the slide. However, a protective plexiglass window was installed a month later in November 2016 before the winter and required the radar to be re-oriented slightly toward the north side of the slope due to both the orientation of the shelter structure itself and in order for the radar to be perpendicular to the window thereby reducing the reflection of radar waves.

The challenges at the site included frequent snowfall in the winter that partially covered the slide area including the rock face at the toe of the slope. The system was initially powered by two 260 W solar panels and a battery pack allowing for 5 to 15 d of monitoring during the fall and winter months, as well as a small gas-powered generator that was used to boost and recharge the battery banks intermittently. The power system was upgraded in October 2018 by installing an additional four solar panels and replacing and upgrading the battery capacity.

Telecom equipment consisting of a cellular modem with an external directional antenna and a power supply connected to the batteries was installed to allow for remote connectivity to the GB-InSAR equipment and data, This upgraded system operated continuously for a maximum of 1.5 months from March to June 2019 and was accessible remotely through VPN, see Table 2.

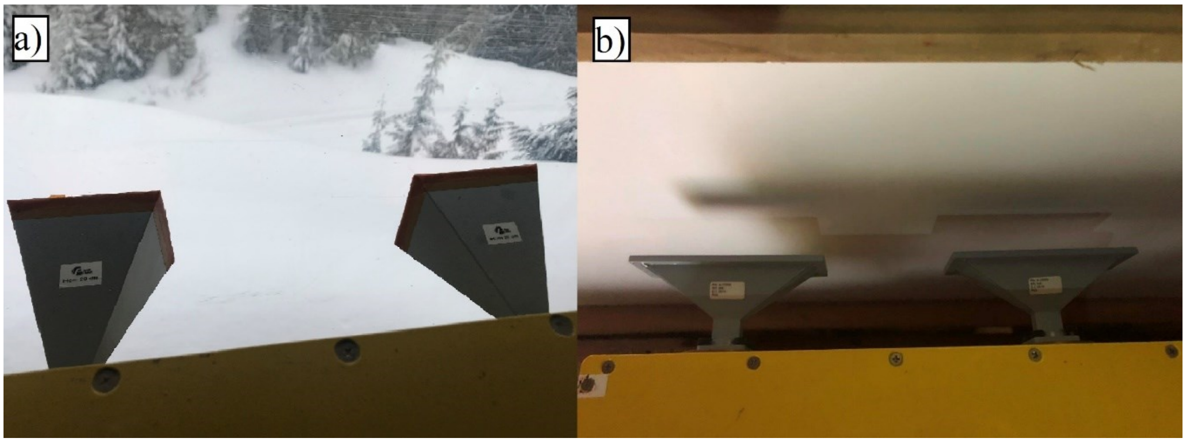

Figure 3-5: Initial radar antennas a) and new wider field-of-view antennas b)

Additional changes to the installation were made in September 2019 through collaboration with BC Hydro and IDS GeoRadar in order to improve the quality and coverage of the radar data. Given the distance to the target slope, slope width, and orientation of the radar shelter, it was evident that the existing spatial coverage of the radar system was not optimal to provide good-quality, reliable measurements over the entire slope area; particularly the south side of the slope and upper vegetated area above the rockface. Therefore, three changes were made to the system that included: replacement of the existing radar head antennas with new wider-angle antennas (Figure 3-5), replacement of the existing plexiglass shelter window with a rohacell foam window that is transparent to the radar frequency (Figure 3-6), and installation of corner point reflectors at key locations on the upper vegetated area of the slope in order to try and improve the coherence in these areas.

Figure 3-6: Protective Rohacell foam window as viewed from outside shelter a) and inside shelter b)

These corner point reflectors were installed either by directly bolting them to a rock face, or by mounting them on an elevated post/tri-pod in order to be above the snowpack in the winter and all pointed toward the radar shelter across the reservoir. These three changes in conjunction with one another have significantly improved the spatial coverage and strength of the radar data returns from the slope (Figure 3-7). However, whether these changes will be successful in improving the ability for the system to monitor the slope in near real-time and deepen the understanding of the slopes deformations patterns and kinematics is yet to be determined until a sufficient dataset with these changes have been collected and subsequently interpreted; as such, this is outside the scope of this paper.

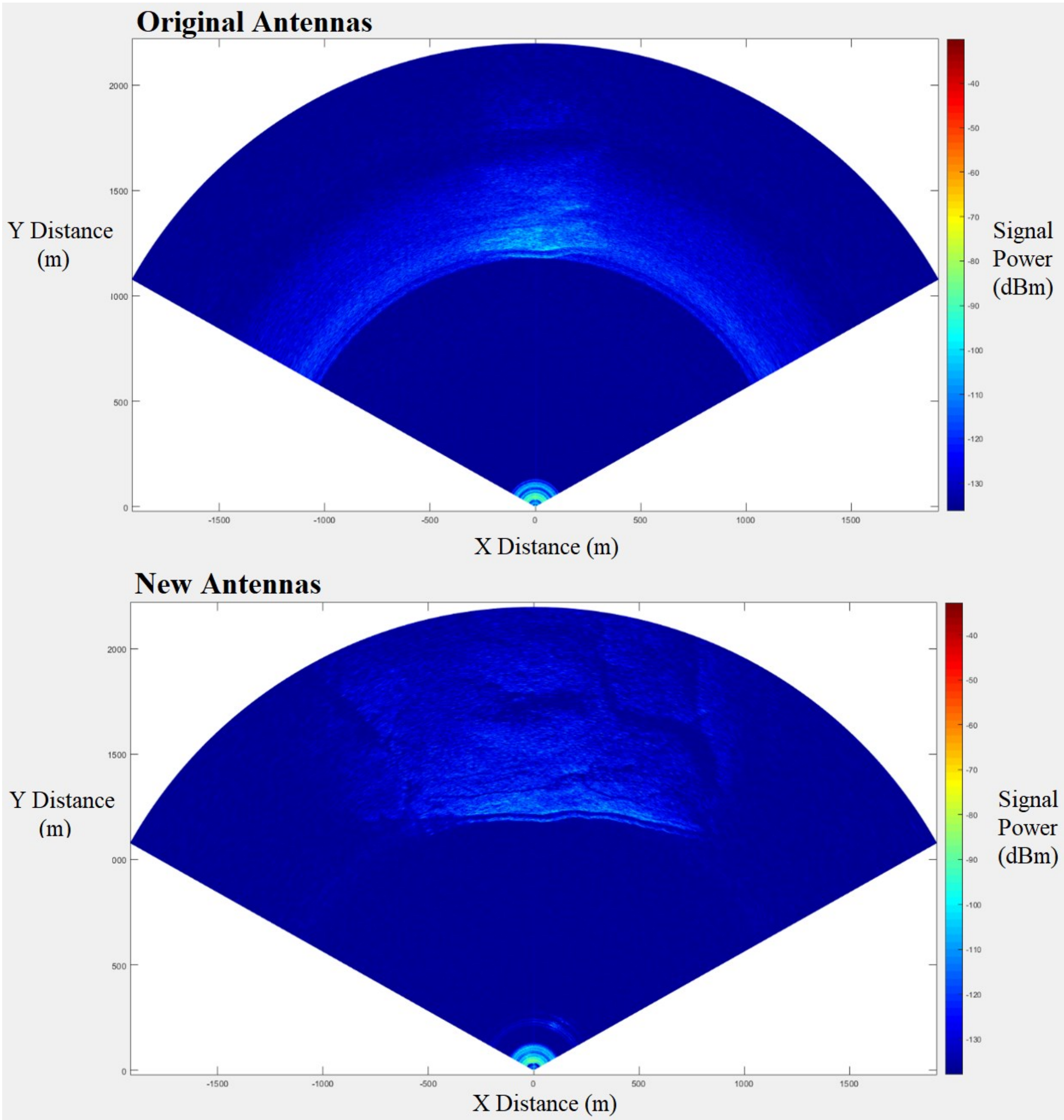

Figure 3-7: Radar signal strength and coverage before a) and after b) installation improvements

3.4.2 Continuous Data (C-InSAR)

Continuous data is typically processed by software supplied with GB-InSAR equipment from the respective manufacturer. In the case of the IBIS-L radar used at this site, IBIS Guardian software provided by IDS Georadar with the equipment was utilized to process field data and could be calibrated to monitor displacements and velocities of selected specific points and/or areas within the study site such as the active zone previously described.

Time-series plots of these points and/or areas can be generated within this software and the inverse-velocity methodologies pioneered by Fukuzono (1985) can be applied to predict and warm of imminent slope failure. Once an adequate set of continuous data has been acquired from this site due to the power and radar system improvements, it could be analyzed and compared to the results of the discontinuous data.

Due to the high temporal frequency of the continuous GB-InSAR data it was anticipated that the data could potentially provide new insights into the seasonal displacement pattern observed at this site and potential triggering mechanisms when compared to piezometric, temperature, and weather data. However, a significantly long dataset would have to be acquired in order to allow enough movement of the slide to be detectable, therefore this analysis is restricted to discontinuous methodologies.

3.4.3 Discontinuous Data (D-InSAR)

During discontinuous data acquisition, GB-InSAR is used during several separate campaigns, revisiting a given site periodically (Monserrat et al. 2014). This methodology is also applied with satellite based InSAR, which acquires data discontinuously between the satellite's orbital return period for a given site. A detailed review of this methodology can be found in Crosetto et al. 2016. The processing and analysis of D-InSAR data poses substantial technical differences compared to C-InSAR data (Monserrat et al. 2014). One of the critical issues with D-InSAR data is obtaining a sufficiently high coherence, as large time gaps can lead to severe coherence loss (Monserrat et al. 2014).

IDS Georadar provided their Repeat Pass software for processing the discontinuous data from Checkerboard Creek. This software takes the best matches from subsequent monitoring campaigns to output a 2D displacement map for locations in the monitored area within a set coherence threshold. This uses the persistent scatters (PS) technique, reviewed in detail in

Colesanti et al. 2002. The maps output from the Repeat Pass tool can then be exported from IDS's Guardian software and aggregated in Esri ArcMap to determine the total cumulative displacement of areas within the radar's field of view. An assumed stable zone to the north of the slide where data coherence is high, was then selected and the displacement data corrected to be relative to this area to compensate for apparent movement due to snow accumulation/melt and other effects. The assumed stability of this area is consistent with regular historical monitoring by BC Hydro. Discussion on the use of this methodology in order to compensate for apparent movements due to snow accumulation and melt at this site is discussed in detail in Woods et al 2020.

3.5 Results

One of the benefits of the use of GB-InSAR for monitoring slopes is its ability to cover a large area in a continuous map of displacement data. In comparison, the existing monitoring at this site consists of separate point-wise data (survey points, slope inclinometers, extensometers etc.) that have spatial gaps that can make it difficult to determine the failure mode, bounds of active zones, unstable blocks, stable areas etc.

3.5.1 Deformation Mode Confirmation (Toppling)

As discussed in previous sections regarding observed slope deformation trends and modelling of this slope; investigations and analyses have largely concluded that the predominant deformation mechanism of this slope is toppling combined with shear on conjugate sub-vertical joint and cross cutting shear (Watson and Moore 2005). However, the types of deformations observed in this slope are not consistent with either pure flexural or block toppling. While some rotation does occur, deformation is complex and occurring on numerous shears and joints which separate the rock mass into separate deformable blocks (Watson and Moore 2005). Under gravitational loading these blocks slip relative to each other resulting in general down dropping and out of the slope dilation.

Given this slope deformation mechanism, where observed slope movements from in-place instrumentation are greatest along the slope surface and diminish with depth and are consistent with rotational toppling (Psutka et al. 1996), apparent deformations based on analysis of the GB-InSAR data is restricted to the slope surface. In addition, high coherence and good quality data returns appear to be currently restricted to the rock cut located at the toe of the slope. However, confirmation of this anticipated deformation mechanism still may be achieved through analysis of the GB-InSAR data by comparing apparent displacements of the crest of the rock cut to the toe of the same area where active movements have been observed. This analysis was completed by defining two respective crest and toe areas within the active zone on the rock cut where radar returns were above a reliable level of coherence and determining the average relative cumulative displacement for each area over the monitoring period. A linear regression trend line and 95% confidence interval was also applied to each dataset based on the number of pixels and standard deviation within each area. This resulted in an average cumulative displacement of approximately 0.7mm and 8.6mm over the monitoring period, for the rock cut toe and crest, respectively (Figure 3-8).

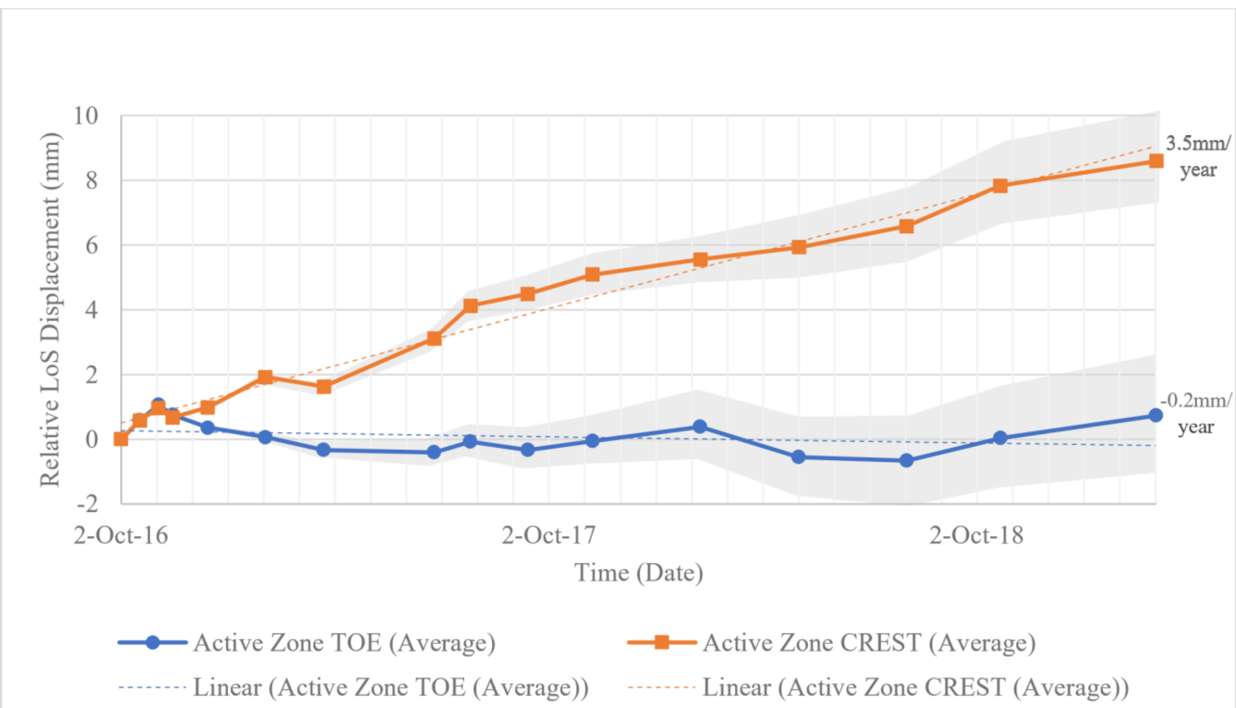

Figure 3-8: Cumulative apparent average displacements of crest and toe of slope rockface

This relates to an average displacement rate of about -0.2mm/y and 3.5mm/y by linear regression of the toe and crest datasets. These average values are generally consistent with those from other in-place instrumentation in the same areas, however, less than the observed maximum displacement rates within the active zone. This is to be anticipated given that this is an average over the entire active area and observed displacements have typically been restricted to the central crest of the active zone. Ultimately, the relative greater apparent displacement rate of the rock cut crest from the GB-InSAR data is consistent with the hypothesized mode of deformation of the slope being complex rotational toppling.

3.5.2 Seasonal Displacement Pattern

The Checkerboard Creek Rock Slope can generally be categorized as an extremely to very slow velocity landslide (WP/WLI 1995; Varnes 1996) based on the maximum displacement rate observed at the site since it was first identified as an area of potential hazard. As discussed in Section 2.5 and 2.6, observed displacements at this site have been characterized by a well-defined seasonal displacement pattern that has been observed at numerous locations at the site and using multiple monitoring techniques. However, this pattern is most pronounced in the multi-point extensometer data from drillholes CC8 and CC10. This displacement cycle observed in the extensometers consists of an active phase occurring in the early autumn to late winter, and a relatively inactive phase with limited to no displacements during the early autumn period (Watson et al. 2004). Analysis of existing instrumentation data and conclusions from numerical modelling discussed previously has largely identified two primary driving mechanisms for slope movement: seasonal changes in groundwater levels and ground temperature, see Figure 3-3.

Initial analysis of slope monitoring data noted that accelerated displacements were sometimes triggered during periods of increasing water pressure in the slope, however, the correlation with piezometric level and/or rate of change of piezometric level is was consistent (Watson et al. 2004). In addition, much of the active zone of the slope is located above the permanently saturated zone. Therefore, it was postulated that transient pressures develop during infiltration, triggering the annual displacement cycle (Watson et al. 2004). Small accelerations in displacement have occurred during exceptionally high rainfall events and/or rapid snowmelts, such as in April 2002

(Figure 3-3). However, this has been observed not to always be the case and accelerations in slope displacements in response to increased infiltration have predominantly been limited to the active months in the fall and winter (Watson et al. 2004). This relatively poor correlation and inconsistencies between ground water pressures and accelerating slope deformations eventually led to consideration of other potential driving forces behind the observed annual displacement cycle.

This resulted in a stronger correlation between seasonal temperature variations in the near surface bedrock of the slope than to groundwater level (Watson et al. 2004). However, despite this strong correlation, data from subsurface thermistors indicate that seasonal changes in temperature only penetrate to a depth of approximately 10m below the existing ground surface; which is much less than the depth of observed movement of about 50m. Therefore, one of the purposes of the discontinuous numerical modelling of the slope was to further analyze the probability that seasonal bedrock temperature changes were in fact a likely cause of the observed displacement pattern. Conclusions made from these analyses largely reinforced this hypothesis (Lorig et al. 2009; Martin et al. 2011).

Even though slope modelling has largely agree with the hypothesis of ground temperature changes as a driving mechanism for slope movement, there has been some concern that the observed displacement pattern within the extensometers may instead be due to thermal expansion and contraction of the steel extensometer rods themselves and therefore not entirely representative of the slope displacement. There is some indication of this as the extensometer data has apparent negative ie. backward/upslope movements during dormant periods that are considered unrealistic. Comparing the extensometer to the IPI data, which are installed at a much greater depth that is considered isothermal and therefore note thermally affected, shows a much more consistent downslope movement with seasonal acceleration in the spring months during snowmelt and groundwater infiltration.

Therefore, as the seasonal displacement pattern has been restricted to these in-place instruments with higher measurement frequencies and point-wise data (extensometers and IPIs) it was hoped that analysis of the GB-InSAR may further confirm this pattern and/or further define the spatial extent of where the pattern is most well defined on the slope as this method has been used previously by others to determine landslide activity (Cigna et al. 2013). To determine this, several methodologies were utilized. First, apparent cumulative displacements for the area within the radar view with relatively good coherence was determined, and specific locations where high frequency displacement measurements are taken (such as the extensometers in drillhole CC10) were compared to the D-InSAR results. Results of this analysis and validation with in-place instrumentation was discussed in detail in Woods et al. 2020.

Initially, correlation between the D-InSAR results and the displacement pattern appeared to be restricted to apparent displacements accelerating and decelerating at relatively equivalent times in the autumn 2016 and spring 2017 in the vicinity of CC10 as discussed in Woods et al. 2020. However, any further agreement between the seasonal displacement pattern did not appear to be present in the GB-InSAR data.

Table 3-2: Seasonal Variation of GB-InSAR at Select Instrumentation Locations

Time Period (Date)	Drillhole (Instrumentation Type)		
	CC1 (SI)	**CC4 (SI)**	**CC10 (EXT)**
	Apparent LoS Displacement Rate (mm/y)		
Inactive 1 (Sept. 29, 2016 – Nov. 7, 2016)	12.2	19.7	2.4
Active 1 (Nov.15, 2016 – Mar. 25, 2017)	1.5	5.7	4.9
Inactive 2 (May 12, 2017, Nov. 9, 2017)	6.1	13.4	6.1
Active 2 (Jan. 12, 2018 – Mar. 30, 2018)	1.2	17.8	14.8
Inactive 3 (May 2, 2018 – Oct. 24, 2018)	5.4	20.1	6.9
Active Average	1.3	11.8	9.9
Inactive Average	7.9	17.7	5.1

In order to further assess this, other areas of the slope and partial timeframe datasets were analyzed. This included looking at data from other in-place instrumentation such as the slope inclinometers at CC1 and CC4, the average and maximum displacement values within the zone of active movement, and how those values compared between the winter and summer months when the slope was believed to be active and inactive respectively.

Analysis of specific locations within the GB-InSAR data did not result in further agreement between the resulting apparent displacements and the seasonal displacement pattern. Some areas appeared to have greater than average displacement rates during periods that were expected to be inactive, and others while it was active, see Table 3-2: Seasonal Variation of GB-InSAR at Select Instrumentation Locations. GB-InSAR displacement values appeared to be relatively in agreement with the seasonal pattern in the vicinity of CC10 but almost opposite in the vicinity of CC1 and CC4. Therefore, instead of analyzing specific locations with the GB-InSAR data, a more large-scale analysis of the site was carried out, specifically looking at the entirety of the presumed active area of the movements at the center of the slope.

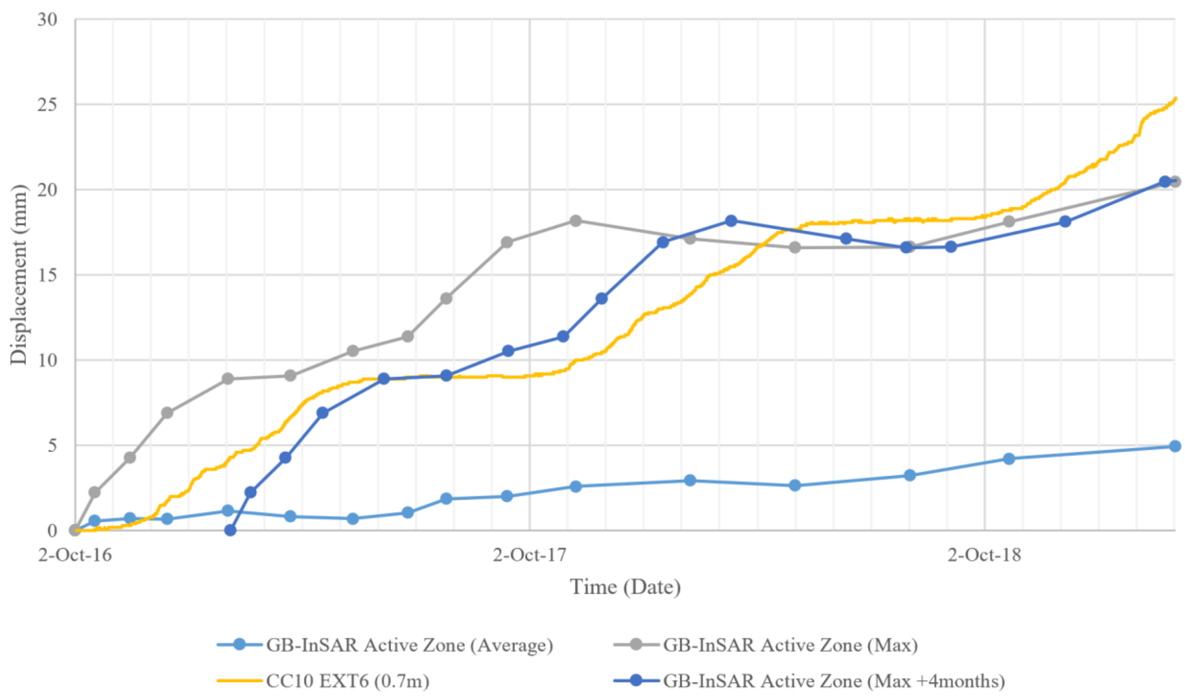

Figure 3-9: Cumulative apparent average and maximum displacements of active zone

The average displacement rate over the whole active zone were relatively low (about 2mm/y, see Figure 3-9), influenced by the cells within the displacement map with little to no apparent movement such as those located at the toe of the slope. In addition, seasonal variation of the average displacement values over the entire active zone appeared to not be present. However, when looking at the maximum GB-InSAR displacement values within the active zone, a seasonal displacement pattern did become apparent, see Figure 3-9. Comparing this seasonal displacement pattern in the GB-InSAR data to that from the high frequency extensometer data from drillhole CC10 over the same monitoring period, the absolute and relative displacement magnitudes over the active and inactive periods do appear to be quite similar. That being said, they don't occur to happen at the same time. Shifting the data by four months appears to create a strong correlation between the datasets, see Figure 3-9.

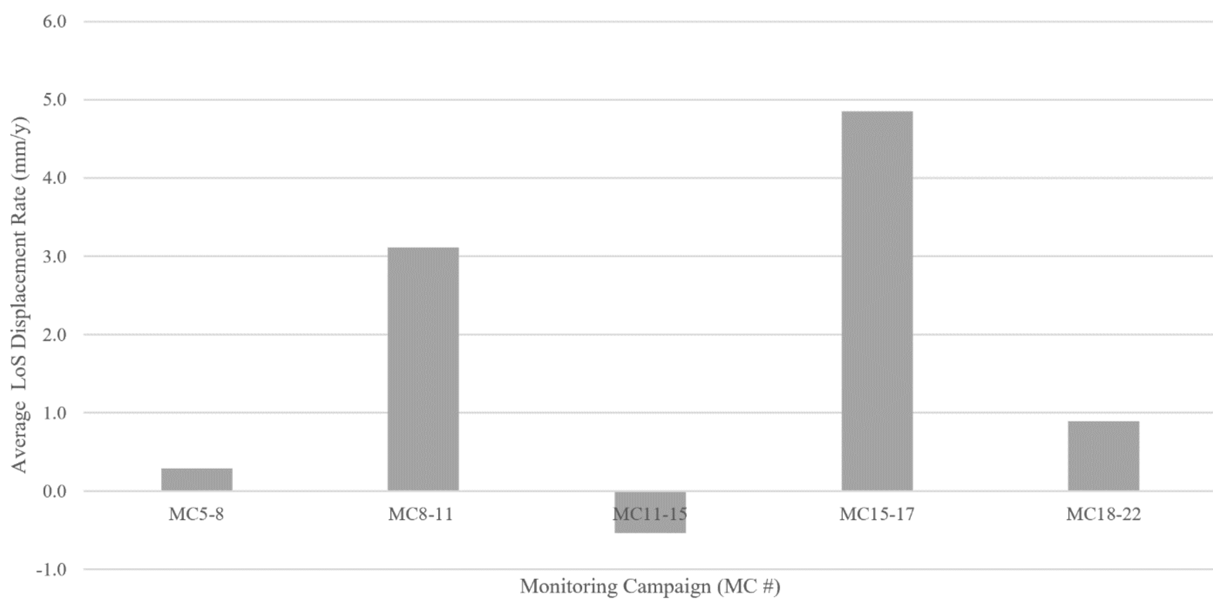

Figure 3-10: Cumulative apparent average and maximum displacements of active zone

Further analysis of the GB-InSAR data for the active zone by combining multiple monitoring campaigns together over subsequent seasonal periods resulted in a similar pattern for the average cumulative rates over those periods, Figure 3-10 and Figure 3-11. This resulted in an average displacement rate of -0.3mm/y for inactive periods and 4mm/y for active periods. However, like the observed pattern from the maximum recorded displacements, this apparent pattern from the average rate also appears to be "lag-behind" or be preceded by the recorded deformations from the in-place extensometers, Figure 3-11. In contrast, comparing this to the IPI data from drillhole

CC3, the seasonal displacement pattern is less well defined but shifted later in the year, toward the spring which has a greater agreement with the seasonal pattern in the GB-InSAR results, see Figure 3-12.

Therefore, the source of this potential delay in recorded apparent movements in the GB-InSAR compared to the extensometer data may be due to the thermal effects within the instrument itself, where displacements recorded by the IPI may considered to be more representative of the actual slope movements. Other sources of this temporal incongruity may be due to several factors such as the discontinuous nature of the dataset, or movements not becoming apparent until after melting of the snowpack in the spring and summer months. Ultimately, analysis of the GB-InSAR by D-InSAR methodologies does seem to reinforce previous observations of seasonal changes in the displacement rate of the slope.

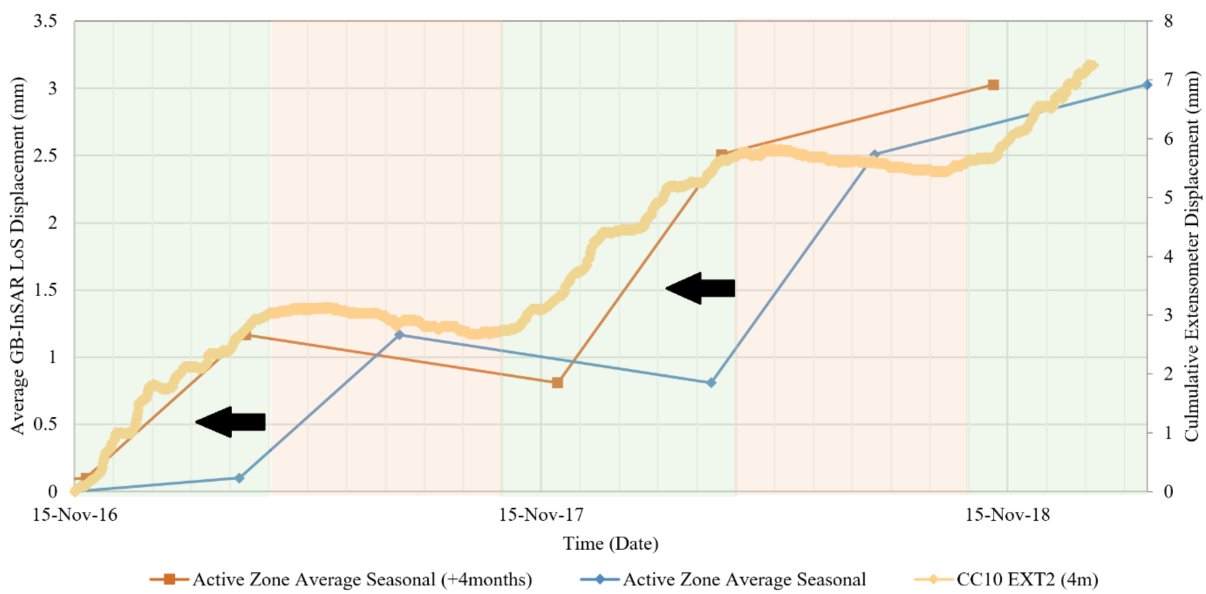

Figure 3-11: Seasonal displacement rate of GB-InSAR results vs. extensometer instrumentation data

When analyzing the displacement rates of certain areas of the slope by looking at the 2D velocity maps generated in ArcMap, some interesting features can be observed, Figure 3-12. For one, these maps generally reinforce the observation that the slope appears to be more active over some periods than others and have some inherent seasonality. Second, that the central area of the slope, where displacements have been recorded to be most active by in-place instrumentation, appear to be relatively active throughout the year, however, accelerate during certain periods. As well, there is some apparent seasonal fluctuations of displacements in other parts of the rock cut including in the vicinity of features referred to as “The Rusty Shear” and “Ballpark” on the north side of the site which is discussed further in the next section. Note that further data collection, analysis, and confirmation of some of these apparent displacements is required before drawing definitive conclusions.

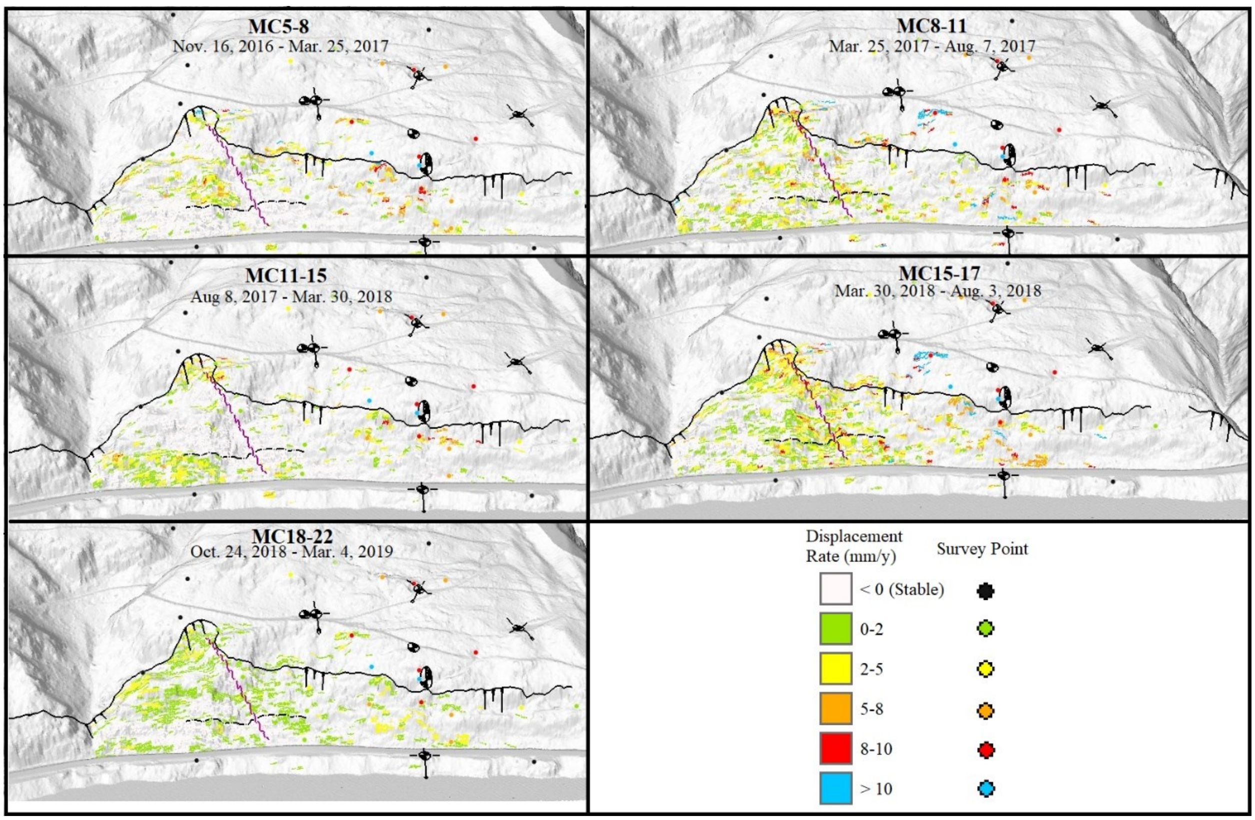

Figure 3-12: GB-InSAR displacement rate maps for separate seasonal periods

3.5.3 Spatial Extent of Active Slope Movement

While the upper, eastern bound of the area of active movement at the Checkerboard Creek Rock Slope is fairly well defined by the observed tension cracks, other surface features, and displacement data from existing in-place instrumentation, the other bounds to are less well-defined. The western, downslope boundary of the active area is generally considered to be near the toe of the rock cut for the Hwy, however, may extend beyond this point, below the water level of the reservoir. The GB-InSAR signal is unable to penetrate the water surface and therefore is unable to provide any insight into the location of this boundary. In addition, due to the current orientation of the radar toward the north side of the slope, and the relatively narrow field-of-view of the older antennas, the majority of the data available does not cover the southern side of the slope in reliable radar returns. Due to this, there is limited ability to determine the southern lateral boundary of the active area of the slope.

By order of elimination, this leaves the northern lateral boundary of the active zone that analysis of the GB-InSAR data may provide additional insight into its extent. Previous analyses of existing monitoring data and site surveys indicated that the northern boundary of the active zone may be in the vicinity of a steep fault zone feature on the rockface located to the north referred to as the "Rusty Shear" as indicated in Stewart et al. 2002 and Psutka et al. 1999. Plan drawings and figures of the site show this feature as a mapped fault and area of closely spaced fractures located within the gneissic granite/granodiorite unit. Psutka et al. 1999 states that the rock south of this zone is moderately to highly weathered whereas it is relatively fresh, although slightly altered. It has been assumed that the areal extent of the moving rock mass is controlled by the weaker rock in the weathered zone of the fault which may be a result of long-term gradual movements (Psutka et al. 1999). One of the strongest indications that this feature represents a potential lateral boundary for the active zone is that the rock mass quality one either side of the Rusty Shear is significantly different with the rock to the north being generally more massive, with fresh un-weathered surfaces , and well defined benches and blast holes from the excavation of the rock cut for the Hwy. In contrast, the rock mass to the south of this feature has had these bench and blast hole features become much less defined since its initial excavation, forming a more uniform slope angle, with more weathered and rusty-colored surfaces (Figure 3-13).

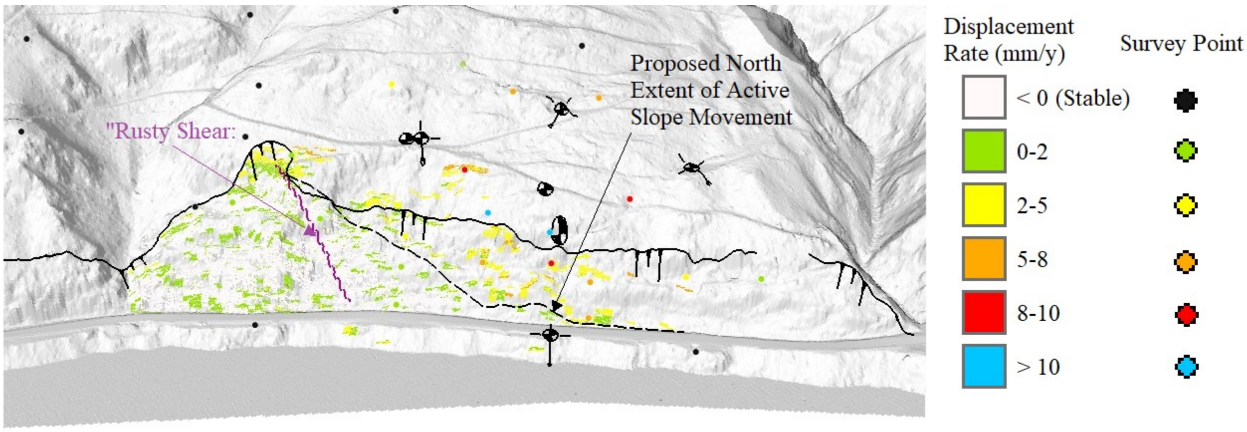

Figure 3-13: GB-InSAR displacement rate map for entire monitoring period and rock cut surficial features

Generally, shear zones like this feature comprise about 15% of the mapped surface discontinuities at this site, and are more concentrated in the lower levels of the highway excavation (Psutka et al. 1999). They vary widely in appearance as a function of surrounding mineralogy and rock fabric and are mostly undulating, contain 1 to 5mm of gouge or breccia, with an assocaited zone of 10 to 50cm of crushed and brecciated rock (Psutka et al. 1999). Specifically, annual surveillance of the site in 2010 by Psutka notes that the Rusty Shear has small chlorite lenses (1 x 4 mm). This area also has had observed surface seepage at numerous occasions that can persist for weeks to a couple of months following snowment (Psutka et al. 1999). These observations along with surface survey and subsurfacen instrumentation displacement patterns in the area have supported the hypothesis that this feature represents the northern lateral boundary of the area of active slope movement.

However, analysis of the D-InSAR results indicate that the northern boundary of the most active part of the slope is located slighty south of the Rusty Shear, more toward the centre of the slope as illustrated in Figure 3-13. This boundary does appear to start in the vicinity of the Rusty Shear at the crest of the rockface and then trends toward the west/toe of the rockface as you move to the south and center of the slope. The average rate dispalcement rate threshold used to determine this potential northern extent of the active boundary is 2-5mm/year, which is indicated by the yellow pixels in Figure 3-13. This is relatively consistent with the displacement rates of the survey points located on the surface in this area (Survey Point M27, M28, and M36) with the apparent average rates in the vicinity of this boundary and south of the Rusty Shear all less than 2mm/y, see Figure 3-13.

In contrast, the GB-InSAR results show that the area to the north of the Rusty Shear, refered to as "The Ball Park" by BC Hydro, has minimal apparent displacements (less than 2mm/y) over the entire monitoring period. That being said, there are two select survey points in this area that do record some apparent movents (M35 and IP101) see Figure 3-12 and Figure 3-13. It is important to note that observations from both site monitoring and modelling have interpretted the northern lateral extent of the active zone as a potentially gradational boundary, with no sharp, well-defined contact between active and inactive zones such as represented in Figure 3-1 and Figure 3-2, and in Stewart et al. 2002. In addition, as discussed in Section 5.1, the displacement rate is generally much lower toward the toe of the slope, meaning displacements toward the base of the Rusty Shear may be quite slow and therefore poorly represented in the GB-InSAR data.

Another surficial feature of note of the north side of the rockface is a narrow ledge that runs parallel to the slope north of the Rusty Shear that has been identified as a potential failure surface, see Figure 3-14. This ledge appears to dip out of the slope at approximately 15 to 20 degrees from the horizontal (Psutka 2010) yet no offest has been idenstified laterally across the structure. The liklehood of this feature as a failure surface is currently considered speculative, with limited avaiable monitoring data.

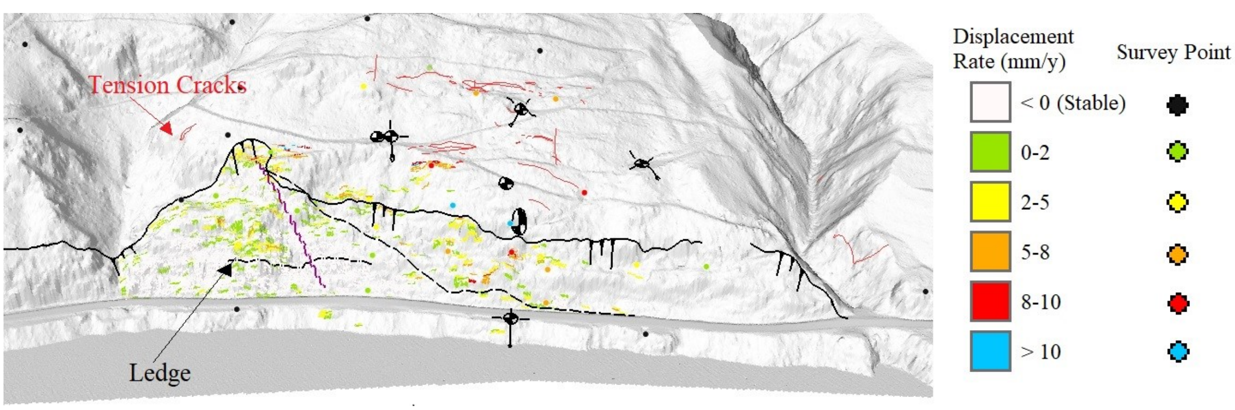

Figure 3-14: GB-InSAR displacement rate map for data subset from MC5 to 12 and mapped tension crack locations

In order to assess this feature as a possible failure surface further analysis of the D-InSAR data was carried out which included analysis of subsets of the data and constructing further time series plots of areas of suspected movement. When restricting the GB-InSAR results to the time period from monitoring campaign (MC) 1 to MC 12 (September 29, 2016 to September 20, 2017) an area of apparent movement north of the Rusty Shear in the center of the Ball Park area can be observed (Figure 3-14). These identified movements appear to be occuring directly upslope of the ledge/possbile failure surface discussed prevoiusly. On average, this area appears to be experiencing relaively slower average displacements of about 0.4mm/y (up to 2.9mm/y maximum), which is much slower than the displacements of the active zone at the center of the slope according to both the GB-InSAR results and historical survey and instrumentation monitoring. The average displacement rate of this pontential active block north of the Rusty Shear is consistent with survey points M35 and IP101 which have an average displacement of approximately 0.6 to 1.5mm/y. However, note that these survey measurements do appear to be quite variable year to year. It is only because these measurements have been recorded over such an extensive period of time (since 1992 at the earliest) that these displacement trends have become apparent given the very slow rate of movement.

This active block may also be responsible for the mapped tension crack to the far north side of the site above Ballpark Creek, see Figure 3-14. Field notes of this tension crack has no signs of recent displacements with significant vegetation cover, and therefore considered largely dormant.

Despite its very slow estimated displacement rate, this potentially active block may represent a significant northward extension of the known extents of the active landslide on this slope and a large increase in the total landslide volume. That being said, the depth and therefore volume of this potentially moving block is not able to be determined due to the nature of the GB-InSAR monitoring being restructed to surficial movements. As such, this may simply represent a shallow, potential rockfall-like hazard feature in contrast to the more consistent downhill movement of the central section of the slope which represents a large mass undergoing complex toppling. This area defined by the GB-InSAR data subset and surrounding survey points may also represent an area of displacement that is independent of the currently defined active zone with a greater periodicity of dormant periods followed by active movements that reactive with greater slope movement to the south. There is some indication in the area of the Ballpark of historical movements that include the absense (or relative lack of definition) of the glacial scour feautures that are well defined across the rest of the site. Topographic features in the area also indicate potential historical failures and erosion.

3.5.4 Upper Vegetated Area of Slope

Initial analysis of the GB-InSAR dataset resulted in some indication that the system was receiving relatively strong radar signal returns from some areas within the upper vegetated (and lower angle) portion of the slope at this site. As such, it was included in the D-InSAR analysis in order to assess the systems capability to monitor slope deformations in this area, where it was felt that the presence of vegetation, lower incidence angle, and generally deeper snowpack may impact the results negatively. Comparing the resulting apparent displacements from the GB-InSAR data in this area with the in-place instrumentation made it clear that the D-InSAR analysis resulted in much greater displacements over time than what was anticipated or recorded by in place instrumentation. This is most likely due to a general lower coherence in these areas which resulted in temporal decorrelation and increased apparent displacement values. As such, results in this area were not believed to be accurate or representative of real displacements and therefore eliminated from the Figures provided. As other monitoring methods on the site have indicated that there is measurable displacements within this vegetated area, further work has been carried out to install corner point reflectors to increase the coherence of the radar signal in this area at strategic points as discussed in Section 3.1

3.6 Conclusions

This paper provides a summary of the successful implementation and analysis of GB-InSAR monitoring technology and data at a natural slope bedrock landslide site known as The

Checkerboard Creek Rock Slope located near Revelstoke, BC. GB-InSAR monitoring of this site has provided high resolution continuous data that has been analyzed in detail to provide new insights and a greater understanding of displacement trends/patterns, triggering mechanisms, and failure kinematics of the landslide in comparison to existing conventional, point-wise, and low-frequency in-place instrumentation.

These insights include further confirmation of the currently understood deformation mechanism of complex rotational toppling, refinement of the norther extent/boundary of the active zone of slope movement, verification of the seasonal variation in displacement rates, and possible identification of new previously unidentified areas of potential movement. Despite these insights, challenges with the installed GB-InSAR system and associated technological limitations persist. Therefore, changes to the system including the installation of new radar antennas, protective foam shelter window, and corner point reflectors have been completed in order to further improve the reliability and performance of the system and improve the overall quality of the resulting data. Further GB-InSAR data collection and analysis including that of long-term continuous datasets and improved quality and spatial coverage of radar signal returns may further validate the insights made by the analysis of the discontinuous datasets obtained from the initial installation configuration.

GB-InSAR monitoring technology offers many advantages when used to complement other techniques including the ability to cover a large area with high-frequency, accurate, continuous displacement data, 24 hours a day, in all weather conditions. Overall, the findings of this research verify the feasibility of implementing GB-InSAR technology such as this to monitor similar slopes even in challenging conditions. In addition, continued monitoring and analysis of new improved datasets may build upon these insights and provide an operational tool for near real-time monitoring of the slope.

4 CONCLUSIONS AND RECOMMENDATIONS

This thesis provides a detailed an overview and assessment of GB-InSAR technology for the purposes of geotechnical slope monitoring and site characterization of natural slopes with challenging conditions. It provides a detailed evaluation of the logistical challenges and technical limitations of the application of this technology in remote mountainous environments that are typical of landslide sites in Canada that includes dense vegetation and seasonal snow-cover and how to address them. This evaluation includes GB-InSAR's advantages and limitations in comparison to both conventional in-place geotechnical instrumentation and other remote sensing monitoring methodologies. By applying this technology at an area of known landslide risk, a detailed site specific analysis was completed that was able to provide further insights into the deformation characteristics of a natural slope bedrock landslide site known as The Checkerboard Creek Rock Slope located near Revelstoke, BC. Readily available and cost-effective solutions were also utilized at this site to successfully address some of the challenges and limitations associated with this monitoring technology.

This technology, and other remote sensing techniques like it, possess several qualities that are potentially advantages in more effectively monitoring actively moving slopes and quantify risk to nearby infrastructure and the public. This goal of this research, therefore, is to assess the efficacy of GB-InSAR when being applied to monitor natural slopes with typical Canadian mountainous environments and how it may best be utilized by geotechnical professionals to mitigate landslide risk and carry out slope stability assessments.

4.1 Resolution of Logistical Challenges of Checkerboard Creek GB-InSAR Installation

The primary logistical challenge associated with the Checkerboard Creek Rock Slope site was insufficient solar power generation for continuous operation of the GB-InSAR equipment. Initially, the equipment was powered by two 260 W solar panels and associated battery pack. This system, which was installed prior to the initial field work associated to this thesis, allowed for 5 to 15 days of slope monitoring, resulting in discontinuous data from October 2016 to March 2019. Therefore, the solar power system at the site was upgraded in October 2019 as part of this research with the installation of four additional 270 W panels and replacing and upgrading the battery capacity with four new 24 V, 100 A battery packs in placed insulated aluminum battery boxes. This upgraded system operated continuously from March to June 2019 and greatly increased the ability of the system to operate with limited requirement for intervention by site staff.

In addition to the upgrade of the onsite power system, a telecommunications system was also installed which consisted of a wireless modem with an external directional antenna and an associated power supply. This allowed for remote connectivity to the GB-InSAR system via VPN software that can be used to download monitoring data for analysis, and operation of the system itself.

Additional improvements to the GB-InSAR installation were made in September 2019 through collaboration with BC Hydro and IDS GeoRadar to improve the data quality and spatial coverage of the radar data. Before these improvements, the coverage of the radar system on the slope was not optimal in order to provide good-quality, reliable measurements over the entire area of interest. This was particularly true for the the south side of the slope and upper vegetated area above the highway rockcut. Therefore, the system's existing radar antennas were replaced with new wider-angle antennas, the existing plexiglass shelter window was replaced with a rohacell foam window that is transparent to the radar frequency, and radar corner point reflectors were installed at key locations on the upper vegetated area to improve the coherence.

These three changes have significantly improved the spatial coverage and strength of the radar signal returns from the slope. However, whether these improvements are successful in improving the ability for the GB-InSAR system to monitor the slope in near real-time is yet to be determined until a sufficient dataset with these changes have been collected and subsequently interpreted.

4.2 Validation of GB-InSAR Results

Due to the restrictions regarding solar power generation during the initial installation of the GB-InSAR at the Checkerboard Creek site, the majority of the data were acquired discontinuously from October 2016 to March 2019. Therefore, the data was processed using discontinuous methodologies with IDS Georadar's Repeat Pass software to compare temporally disparate monitoring campaign datasets. The maps output were aggregated in Esri ArcMap to determine the total cumulative displacement of the slope. An assumed stable zone to the north of the slide was then selected to correct the data to be relative to this assumed stable zone area to compensate for snow accumulation and melt over those time periods.

Initial validation of the GB-InSAR was completed by comparing the average displacement values of pixels from the output map in the vicinity of in-place instrumentation (such as extensometer CC10, slope inclinometer CC4, and nearby survey points) and comparing with both recorded displacements over the same time period and historical averages. This comparison resulted in significant agreement between the GB-InSAR and in-place instrumentation datasets in the area at the toe of the slope near the highway rock cut. This included includes agreement on maximum surficial displacement rates and timing of some slope displacement accelerations.

4.3 Evaluation of Limitations of GB-InSAR (Snow cover & Vegetation)

Overall, this research found that discontinuous GB-InSAR monitoring methodologies, such as the persistent scatterer interferometry processes used, can be feasibly implemented to monitor slopes at landslide sites with deep seasonal snow-cover, given considerations including limitations and logistics are addressed, and compensating for apparent movements due to snow accumulation and melt are done by making displacements relative to a known stable area. However, challenges associated with coherence loss from vegetation continue to be an ongoing challenge in regards to reliably monitoring natural slopes. Therefore, additional measures have been implemented at the Checkerboard Creek Rock Slope site, such as the installation of corner point reflectors in these areas and the replacement of the existing radar antennas with models with a wider field of view and a less reflective foam window, to strengthen the radar signal and increase the data quality.

4.4 Insights into to the Checkerboard Creek Rock Slope Deformation Characteristics

The GB-InSAR system at this site was used to provide further insights and understanding of slope displacement trends, triggering mechanisms, and failure kinematics of the landslide when compared to data from existing conventional, point-wise, and low-frequency in-place instrumentation. The insights gained through the implementation of this tool included further confirmation of the currently understood deformation mechanism of complex rotational toppling without a well-defined sliding surface. In-place instruments suggesting higher rates of deformation at the crest of the rock cut as opposed to its toe were confirmed by the displacement map obtained with the GB-InSAR. More importantly, the monitoring data allowed refinement of the northern extent of the most active zone of slope movement, for a threshold rate of 2 mm/y, which allows confirmation of the estimated volume of material showing the most activity (2 million m^3) which poses risk to the nearby Revelstoke Dam. The value of the implementation of GB-InSAR monitoring at this site and potentially others like it is demonstrated by the identification of a potential unstable block north of the most active area, as interpreted from previous analyses. This last insight requires further investigation and continued monitoring.

Previous understanding of slope deformation patterns from near-surface extensometer instruments and previously completed numerical modelling were considered to be associated with near-surface ground temperature changes which onset accelerated periods of slope movement. In contrast, the effect of seasonal changes in transient ground water pressures observed in deeper instrumentation, located well outside the zone of thermal influence, was considered a secondary effect. However, GB-InSAR monitoring results do not show the same seasonality of deformations measured by near-surface in-place instruments (such as the extensometers) which suggests that thermal effects on near-surface in-place instruments themselves, not actual ground movements, may have a greater influence on the observed seasonal than previously recognized and may explain anomalous backward or upslope movement recorded during warmer summer months while extensometer rods would lengthen due to thermal expansion. Therefore, this analysis indicates that increased groundwater piezometric levels due to infiltration from spring rain and snowmelt have a greater influence on inducing slope movement when comparted to changes in seasonal ground temperatures. This could then provide critical insights into the landslide triggering mechanism when considering potential mitigation options, such as installation of additional slope drainage or redirection of surface run-off.

4.5 Recommendations for Further Research

The detailed assessment and analysis of the GB-InSAR data initially collected by the system installed at the Checkerboard Creek Rock Slope demonstrated both its ability to monitor slope movements but also revealed its short-comings as it was initially installed. As such, significant time, effort, and investment was made to further improve the overall operation of the system and resulting data quality as part of this research. However, sufficient time has not yet passed since these improvements have been made to allow for collection of new slope displacement data and subsequent interpretation. In addition, despite the insights provided by the currently available data, further questions regarding the site slope movements and failure mechanism(s) have yet to be fully answered.

Before any further research is initiated, it is recommended that some additional minor improvements are made to the GB-InSAR system, including replacement of the currently ruggedized laptop installed at site with an updated equivalent with an updated operation system (Windows 10, for example) and importantly the ability to re-boot automatically after the loss of electrical power and compatibility with current VPN software for remote access. In addition, a separate data processing computer should be set-up at BC Hydro's offices or approved third-party site to remotely and automatically download, store, and process the collected GB-InSAR data. When these changes have been made the system should be operating optimally as to collect long-term continuous data at the highest possible quality and accuracy.

Further research should be initiated to take advantage of the recent investment made in the system and resulting data improvements. Two primary areas of future research are recommended: first, quantitative analysis and assessment of how the changes made to the GB-InSAR system have affected the data quality and coverage including the changes to the radar antennas, protective window, and corner point reflector installation. Limited literature or case studies regarding how either window materials or the use of corner point reflectors impact GB-

InSAR monitoring results, especially in heavily vegetated and snow-covered terrain. Second, analysis of the new continuous GB-InSAR datasets with improved quality and coverage should be completed to answer questions such as establishing a southern lateral extent of the active zone of slope movements and further assessment of the observed seasonal displacement pattern and failure mode.

References

Atzeni C, Barla M, Pieraccini M, Antolini F (2014) Early warning monitoring of natural and engineered slopes with ground-based synthetic-aperture radar. Rock Mech Rock Eng 48(1):235-246

Barla G, Antolini F, Barla M, Mensi E, Piovano G (2011) Ground-Based Radar Interferometry (GBInSAR) for the monitoring of a deep-seated landslide (Aosta Valley, NW Italian Alps), Dipartimento di Ingegneria Strutturale e Geotecnica, Politecnico di Torino, corso Duca degli Abruzzi 24, 10129 Torino (Italy)

Barla M, Antolini F (2015) An integrated methodology for landslides' early warning systems. Landslides 13:215-228

Blown I G (1966) A geological investigation of the Downie Slide near Revelstoke, British Columbia, B. ASc thesis, Department of Geology, University of British Columbia, Vancouver, BC

Burgmann R, Rosen PA, Fielding EJ (2000) Synthetic aperture radar interferometry to measure Earth's surface topography and its deformation. Annu. Rev. Earth Planet Sci. 28: pp 169-209

Canuti P, Casagli N, Ermini L, Fanti R, Farina P (2004) Landslide activity as a geoindicator in Italy: significance and new perspectives from remote sensing. Environmental Geology 45:907-919

Carlà T, Farina P, Intrieri E, Casagli N (2018) Integration of ground-based radar and satellite InSAR data for the analysis of an unexpected slope failure in an open-pit mine. Engineering Geology 235, pp 39-52

Carlà T, Tofani V, Lombardi L, Raspini F, Bianchini S, Bertolo D, Thuegaz P, Casagli N (2019) Combination of GNSS, satellite InSAR, GBInSAR remote sensing monitoring to improve the understanding of a large landslide in high alpine environment. Geomorphology 335, pp 62-75

Casagli N, Farina P, Leva D, Nico G, Tarchi D (2003) Ground-based SAR interferometry as a tool for landslide monitoring during emergencies. Proceedings of IGARSS 2003, 21-25 July 2003, Toulouse, France, pp 2924-2926

Cigna F, Bianchini S, Casagli N (2013) How to assess landslide activity and intensity with Persistent Scatterer Interferometry (PSI): The PSI-based matrix approach. Landslides 10:267-28

Colesanti C, Wasowski J (2006) Investigating landslides with space-borne synthetic aperture radar (SAR) interferometry. Eng Geol 88:173-199

Corsini A, Farina P, Antonello G, Barbieri M, Casagli N, Coren F, Guerri L, Ronchettri F, Sterzai P, Tarchi D (2007) Space-borne and ground-based SAR interferometry as tools for landslide hazard management in civil protection. International Journal of Remote Sensing, 27:12, 2351-2369

Crosta GB, di Prisco C, Frattini P, Frigerio G, Castellanza R, Agliardi F (2013) Chasing a complete understanding of the triggering mechanisms of a large rapidly evolving rockslide. Landslides 11(5):747-764

Crosetto M, Monserrat, Cuevas-Gonzalez M, Devanthery N, Crippa B (2016) Persistent Scatterer Interferometry: A review. ISPRS Journal of Photogrammetry and Remote Sensing 115: 78-89

Dick GJ, Eberhardt E, Cabrejo-Lievano AG, Stead D, Rose ND, (2015) Development of an early-warning time-of-failure analysis methodology for open-pit mine slopes utilizing ground-based slope stability radar monitoring data. Canadian Geotechnical Journal 52: 515-529

Dehls J, Giudici D, Farina P, Martin D, Froese C (2010). Monitoring Turtle Mountain using ground-based synthetic aperture radar (GB-InSAR). GeoCalgary 2010, Calgary, AB, Canada, pp 1635-1640

Ferretti A, Monti-Guarnieri A, Prati C, Rocca F, Massonnet D (2007) InSAR processing: A mathematical approach (part C). In: Fletcher K (ed) InSAR principles: Guidelines for SAR interferometry processing and interpretation, ESA Publications, Noordwijk, pp 120-234

Fey C, Wichmann V (2016) Long-range terrestrial laser scanning for geomorphological change detection in alpine terrain – handling uncertainties. Earth Surf Process Landforms 42:789-802

Frodella W, Cimapalini A, Bardi F, Salvatici T, Di Traglia F, Basile G, Casagli N (2017) A method for assessing and managing landslide residual hazard in urban areas. Landslides 15(2):183-197

Fukozono T (1985) A new method for predicting the failure time of a slope. Proceedings of IVth International Conference and Field Workshop on Landslides, Tokyo, Japan, 23-31 August 1985

Gomez F, Rosenblad B, Loehr E, Smoot J, Lowry B (2019) Long-term monitoring of a slow moving landslide before and after remediation using ground-based radar interferometry. Proceedings of 2019 ASCE Geo-Congress GSP 311

Hutchinson J, Lato M, Gauthier D, Kromer R., Ondercin M, van Veen M, Harrap R (2015). Applications of remote sensing techniques to managing rock slope instability risk. GeoQuebec 2015

Intrieri E, Di Traglia F, Del Ventisette C, Gigli G, Mugnai F, Luzi G, Casagli N (2013) Flank instability of Stromboli volcano (Aeolian Islands, Southern Italy): Integration of GB-InSAR and geomorphological observations. Geomorphology 201:60-69

International Geotechnical Society's UNESCO Working Party on World Landslide Inventory (WP/WLI) (1995) A suggested method for describing the rate of movement of a landslide. Bull Inter Assoc Eng Geol 52:75–78

Jaboyedoff M, Oppikofer T, Abellán A, Derron MH, Loye A, Metzger R, Pedrazzini A (2012). Use of LIDAR in landslide investigations: a review. Natural Hazards 61(1): 5–28

Journault J (2017) Analysis of Modern Landslide Deformations in the Thompson River Valley using InSAR. Department of Civil and Environmental Engineering: University of Alberta

Kjekstad O, Highland L (2009) Economic and Social Impacts of Landslides. In: Landslides–disaster risk reduction. Springer, Berlin Heidelberg, pp. 573–587

Kromer R, Abellan A, Hutchinson D, Lato M, Chanut MA, Dubois L, and Michel J (2017). Automated terrestrial laser scanning with near-real-time change detection – monitoring of the Sechilienne landslide. Earth Surf. Dynam. 5, 293 – 310.

Lane LS (1984) Brittle deformation in the Columbia River Fault Zone near Revelstoke, Southeastern British Columbia. Can J Earth Sci 21:584-598

Lombardi L, Nocentini M, Frodella W, Nolesini T, Bardi F, Intrieri E, Carlà T, Solari L, Dotta G, Ferrigno F, Casagli N (2017) The Calatabiano landslide (southern Italy): Preliminary GB-InSAR monitoring data and remote 3D mapping. Landslides 14(2):1-12

Lorig LJ, Watson AD, Martin CD, Moore DP (2009) Rockslide run-out prediction from distinct element analysis. Geomehcanics and Geoengineering: An International Journal Vol..4 No.1: 17-25

Luzi G, Crosetto M, Monserrat O (2010) Advanced techniques for dam monitoring. In Proceedings of the 2nd International Congress on Dam Maintenance and Rehabilitation, Zaragoza, Spain, pp 1103-1108

Macciotta R, Martin CD, Morgenstern NR, Cruden DM (2016) Development and application of a quantitative risk assessment to a very slow moving rock slope and potential sudden acceleration. Landslides 13(4):765-785

Macciotta R, Martin CD, Stewart T, Marsh M (2018) Challenges of deploying ground-based InSAR in remote areas in Canada – Trial study and preliminary results. Geohazards 7, Canmore, AB, Canada, June 2018

Macciotta R (2013) Quantitative Risk Assessment of Natural and Cut Slopes: Measuring Uncertainty in the Estimated Risk and Proposed Framework for Developing Risk Evaluation Criteria. Department of Civil and Environmental Engineering: University of Alberta

Martin CD, Alzo'ubi AK, Cruden D (2011) Progressive Failure Mechanisms in a Slope Prone to Toppling (2011) Slope Stability 2011: International Symposium on Rock Slope Stability in Open Pit Mining and Civil Engineering

Matteo L, Romeo S, Kieffer DS (2017) Rock fall analysis in an Alpine area by using a reliable integrated monitoring system: Results from the Ingelsberg slope (Salzburg Land, Austria). Bull Eng Geol Environ 76(2):413-420Monserrat O, Crosetto M, Luzi G (2014) A review of ground-based SAR interferometry for deformation measurement. ISPRS Journal of Photogrammetry and Remote Sensing 93: 40-48

Moore, D (1999) Rock slopes and reservoirs – lessons learned. BC Hydro, Power Supply Engineering, Burnaby BC

Moore D, Wilchek LA, Kroeker MG (2001) Columbia River – Revelstoke Project: Checkerboard Creek Rock Slope – Summary of Information Information for Advisory Board Meeting No. 1. Internal BC Hydro Report No. PSE394

Noferini L, Mecatti D, Macaluso G, Pieraccini M, Atzeni C (2009) Monitoring of belvedere glacier using a wide angle GB-SAR interferometer. J Appl Geophys 68(2):289-293

Peppa M, Mills J, Moore P, Miller P, and Chambers J (2018) Automated co-registration and calibration in SfM photogrammetry for landslide change detection. Earth Surf. Process. Landforms 41 (1): 287-303

Pieraccini M, Miccinesi L (2019) Ground-based interferometry: a bibliographic review. Remote Sens 11(9), 1029.

Psutka JF, Baker DG, Hutchison BJ, Moore DP (1996) Columbia River – Revelstoke Project: Checkerboard Creek Geotechnical Summary Report. BC Hydro Maintenance, Engineering, and Projects internal report. Report No. H2800

Psutka JF (2010) Inter-office memo: Revelstoke Dam – Reservoir Slopes, Checkerboard Creek Rockslope, 2010 Annual Surveillance. Remondino F, Spera MG, Nocerino E, Menna F, Nex F (2014) State of the art in high density image matching. The Photogrammetric Record 29(146): 144–166.

Rosenblad BL, Gomez F, Loehr JE, Legarsky J, Jenkins SM, Held B (2013) Ground-based interferometric radar for monitoring slopes and embankments. Proceedings of 2013 ASCE Geo-Congress

Rott H, Scheuchl B, Siegel A, Grasemann B (1999) Monitoring very slow slope movements by means of SAR interferometry: A case study from a mass waste above a reservoir in Otztal Alps, Austria. Geophys Res Lett 26(11):1629-1632

Salmon GM (1988) A brief introduction to the Revelstoke Project. Can J Civ Eng 15:784–798

Scaioni M, Marsella M, Crosetto M, Tornator V, Wang J (2018) Geodetic and remote-sensing sensors for dam deformation monitoring. Sensors 18:3682

Severin J, Eberhardt E, Leoni L, Fortin S (2014) Development and application of a pseudo-3D pit slope displacement map derived from ground-based radar. Eng Geol 181:202-211

Schulz W, Coe JA, Ricci PP, Smoczyk GM, Shurtleff BL, Panosky J (2017) Landslide kinematics and their potential controls from hourly to decadal timescale: insights from integrating ground-based InSAR measurements with structural maps and long-term monitoring data. Geomorphology 285, pp. 121-136

Snavely N, Seitz SM, Szeliski R (2008) Modeling the world from Internet photo collections. International Journal of Computer Vision 80(2): 189–210

Spaans K, Hooper A (2016) InSAR processing for volcano monitoring and other near-real time applications. J Geophys Res Solid Earth 121:2947-2960

Stewart TW, Moore DP (2002) Displacement behaviour of the Checkerboard Creek rock slope, Terrain Stability in the Interior of British Columbia, BC Ministry of Forests Technical Report 003

Tarchi D, Rudolf H, Luzi G, Chiarantini L, Coppo P, Sieber AJ (1999) SAR interferometry for structural changes detection: A demonstration test on a dam. Proceedings of IGARSS ’99, Hamburg, Germany, pp 1522-1524

Tarchi D, Casagli N, Fanti R, Leva DD, Luzi G, Pasuto A, Silvano S (2003) Landslide monitoring by using ground-based SAR interferometry: An example of application to the Tessina landslide in Italy. Eng Geol 68(1):15-30

Tarchi D, Antonello G, Casagli N, Farina P, Fortuny-Guasch J, Guerri L, Leva D (2005) On the use of ground-based SAR interferometry for slope failure early warning: The Cortenova rock slide (Italy). In Landslides: Risk Analysis and Sustainable Disaster Management, pp 337-342

Taylor H, Lou JK (1983) Design and construction of Revelstoke earthfill dam. Can Geotech J 20:416–427

Travelletti J, Delacourt C, Allemand P, Malet JP, Schmittbuhl J, Toussaint, R, Bastard M. (2012) Correlation of multi-temporal ground-based optical images for landslide monitoring: application, potential and limitations. ISPRS Journal of Photogrammetry and Remote Sensing70: 39–55.

Varnes DJ, Savage W (eds.) (1996) The Slumgullion earth flow: a large-scale natural laboratory. U.S. Geological Survey Bulletin 2130

Wasowski J, Bovenga F (2014) Investigating landslides and unstable slopes with satellite multi temporal interferometry: Current issues and future perspectives. Eng Geol 174:103-138

Watson AD, Psutka JF, Stewart TW, Moore DP (2007) Investigations and Monitoring of Rock Slopes at Checkerboard Creek and Little Chief Slide. Proceedings of 1st Canada-US Rock Mechanics Symposium

Watson AD, Moore DP (2005) BC Hydro Dam Safety Engineering Report E395: Revelstoke Dam Checkerboard Creek Rock Slope Deficiency Investigation Report

Watson AD, Martin CD, Moore DP, Stewart TW, Lorig LJ (2006) Integration of geology monitoring and modelling to assess rockslide risk. Felsbau 24(3):50-58

Watson AD, Moore DP, Stewart TW (2004) Temperature influence on rock slope movements at Checkerboard Creek. Proceedings of the 9th International Symposium on Landslides: Evaluation and Stabilization, 28 June-2 July 2002, Rio de Janeiro, Brazil, pp 1293-1298

Whitehead K, Morrman B, Wainstein P, (2010) The Use of Ground-Based Photogrammetry and SAR Interferometry to Characterize the Surface Motion of an Arctic Glacier. GeoCalgary 2010, Calgary, AB, Canada, pp 1298-1306

Woods A, Hendry MT, Macciotta R, Stewart T, Marsh J (2020) GB-InSAR monitoring of vegetated and snow-covered slopes in remote mountainous environments. Landslides. Published online 04 May, 2020 DOI 10.1007/s10346-020-01408-4

Woods A, Hendry MT, Macciotta R, Stewart T, Marsh J (Submitted) Updated understanding of the deformation characteristics of the Checkerboard Creek rock slope in Canada, through GB-InSAR monitoring

Xie M, Huang Jia, Wang L, Huang Jie, Wang Z (2016) Early landslide detection based on D-InSAR technique at the Wudongde hydropower reservoir. Environ Earth Sci 75:717